

ENGINEERING RESEARCH INSTITUTE  
THE UNIVERSITY OF MICHIGAN  
ANN ARBOR

Technical Report

NATURAL FREQUENCIES IN BENDING OF  
TWISTED ROTATING BLADES

G. Isakson  
J. G. Eisley

Department of Aeronautical Engineering

ERI Project 2582

NATIONAL ADVISORY COMMITTEE FOR AERONAUTICS  
CONTRACT NO. NAW-6490  
WASHINGTON, D. C.

April 1958

## SUMMARY

The effect of twist on the natural frequencies of uniform and tapered non-rotating blades and the effect of twist and blade angle on the natural frequencies of rotating uniform blades are shown by means of charts. Both cantilever and articulated blades are considered. Offset of the root support from the axis of rotation is also considered.

The Rayleigh-Southwell procedure for determining the effect of rotation on natural frequencies of beam vibration is evaluated with respect to twisted rotating blades and found to provide a useful approximation only in certain cases.

A relation developed by Lo and Renbarger for the effect of blade angle on the natural frequencies of a rotating blade is found to provide a useful approximation, under some circumstances, in the case of the fundamental frequency of a twisted cantilever blade.

## INTRODUCTION

The seriousness of the rotor-vibration problem in rotating-wing aircraft usually necessitates a fairly accurate knowledge of natural frequencies of blade vibration at the design stage. It is, consequently, desirable that efficient means be available for the estimation of these frequencies.

While several analytical methods have been developed in this area, they all involve lengthy computation procedures and can be applied efficiently only by the use of automatic digital computing machinery. They are thus not well-suited for use at a preliminary stage of design.

A simplified procedure has been developed for the rapid estimation of flap-wise bending frequencies of rotating blades for the case of zero built-in twist and blade angle.<sup>1</sup> The application of this procedure is, however, not restricted to untwisted blades, but may be extended to blades with moderate amounts of twist, such as have been common in most helicopters in the past. It has been found that the effect of twist, in these cases, is not significant.

The current and projected development of high-performance rotary-wing aircraft, including convertible aircraft, is bringing with it a trend toward substantially increased amounts of built-in twist of the rotor blades, to the extent that the effect of twist is no longer negligible. Under these circumstances, it is desirable that simplified procedures of more general applicability, including the effect of twist, be available for the estimation of blade frequencies. The present investigation was undertaken to satisfy this need.

While a generalized treatment of the twisted-blade vibration problem for combined torsional and bending motion is available,<sup>2</sup> it was decided to limit present consideration to bending alone to avoid introducing at one time an excessively large number of additional parameters.

The objectives of the program were (1) to develop simple approximate procedures for the rapid estimation of natural frequencies of blade vibration, and (2) to determine the effect of parametric variations on these frequencies and so provide background information of value in design. Because of the complex nature of the problem, particularly the coupling effects introduced by twist, the first objective has been only partially achieved; however, much information has been obtained in pursuit of the second objective.

The principal simplification investigated was that involved in the use of the Rayleigh method to predict the natural frequencies of a rotating beam from

a knowledge of the corresponding natural frequencies and mode shapes of the non-rotating beam. This method has been found to provide a good approximation in the case of untwisted beams.<sup>1</sup> In the present work, its application to twisted beams is evaluated.

Another simplification evaluated involves the application to twisted blades of a relation developed by Lo and Renbarger for the effect of blade angle on the frequencies of rotating untwisted blades.

To provide a basis for these evaluations and to provide information on the effect of parametric variations, it was necessary to perform extensive computations using a more accurate method. A number of such methods are available.<sup>3-8</sup> It was decided, after considerable investigation, that the method best suited to the needs of the program and to the available computing machinery was one developed by Targoff,<sup>8</sup> representing an adaptation of the familiar Holzer-Myklestad method to include the effects of twist and rotation. An outline of this method, as modified in the present work, is presented in the Appendix.

The coordinates of the blade are shown in Fig. 2. The x-axis is coincident with the undeformed elastic axis, which is assumed to be straight and to lie in a plane normal to the axis of rotation, and which is in turn assumed to be coincident with the axis of centroids of blade cross sections. The z-axis lies along the axis of rotation, and the y-axis is normal to the x-z plane and positive towards the leading edge of the blade. The nomenclature and sign convention for displacements, shears, and bending moments are illustrated in Fig. 2. Moment vectors conform with the conventional right-hand rule.

In addition to the blade properties and parameters pertinent to the problem of free vibrations of rotating untwisted blades at zero blade angle, namely, spanwise distribution of mass and of stiffness about the major principal axis of the cross section, type of root support, and rotational velocity, the following properties and parameters enter the problem when the blade is twisted: spanwise distribution of stiffness about the minor principal axis of the cross section, blade twist, and blade angular setting with respect to the plane of rotation.

The data may be suitably generalized by expressing all properties and parameters in nondimensional form. Vibration frequencies and rotational velocity are nondimensionalized in the present work by multiplication by the quantity  $\sqrt{\rho_0 R^4 / EI_1}$ . Two types of mass and stiffness distribution are considered, one in which the mass and stiffnesses (both  $EI_1$  and  $EI_2$ ) are uniform, and the other in which the mass and stiffnesses taper linearly to zero at the tip. The latter distribution is considered only in the case of zero rotational velocity. The relative stiffness of the blade about the major and minor principal axes of the cross section is taken into account by means of the parameter  $\gamma$ . Two types of root support are considered, namely, cantilever and fully articulated, and this support is considered to be located at the axis of rotation and, additionally, offset 5% of the rotor radius from the axis of rotation.

## SYMBOLS

|                          |  |
|--------------------------|--|
| $e$                      | offset of root support from axis of rotation   |
| $\bar{e}$                | $e/R$  |
| $l$                      | length of blade segment  |
| $\bar{l}$                | $l/R$  |
| $m$                      | mass of blade segment  |
| $p_1$                    | $\sqrt{T/EI_1}$  |
| $p_2$                    | $\sqrt{T/EI_2}$  |
| $s$                      | coordinate in negative direction of x-axis measured from outer end of beam segment   |
| $x$                      | coordinate in direction of x-axis measured from axis of rotation   |
| $\bar{x}$                | $x/R$  |
| $EI_1, EI_2$             | bending stiffness about major and minor principal axis of cross section, respectively  |
| $\bar{EI}_1, \bar{EI}_2$ | $EI_1/EI_{10}$ and $EI_2/EI_{20}$ , respectively   |
| $K_n$                    | Southwell coefficient for $n^{\text{th}}$ natural frequency [see Eq. (5)]  |
| $M_1, M_2$               | bending moment about major and minor principal axes of cross section, respectively, when centrifugal tension is assumed to act along undeformed position of elastic axis |
| $R$                      | rotor radius   |
| $T$                      | centrifugal tension, $\int_x^R \Omega^2 e \, dx$   |
| $T_1$                    | $\int_x^R \rho \, dx$  |
| $\bar{T}$                | $\int_{\bar{x}}^1 \bar{\rho} \, d\bar{x}$  |
| $V_1, V_2$               | shearing force in the direction of the minor and major principal axes of the cross section, respectively   |

|                          |  |
|--------------------------|--|
| $\beta$                  | angle between major principal axis of cross section and plane of rotation  |
| $\Delta\beta$            | increment in $\beta$ between blade segments  |
| $\gamma$                 | $EI_{10}/EI_{20}$  |
| $\delta_y, \delta_z$     | displacement of elastic axis in y- and z-directions, respectively  |
| $\delta_1, \delta_2$     | displacement of elastic axis in the direction of the minor and major principal axes of the cross section, respectively |
| $\theta$                 | total twist in blade between $x = 0$ and $x = R$ ( $= R\beta'$ )   |
| $\lambda$                | $\omega \sqrt{\rho_0 R^4 / EI_{10}}$   |
| $\mu$                    | $\Omega \sqrt{\rho_0 R^4 / EI_{10}}$   |
| $\rho$                   | mass per unit length of blade  |
| $\bar{\rho}$             | $\rho / \rho_0$  |
| $\phi_{y_n}, \phi_{z_n}$ | displacements in y- and z-directions describing shape of $n^{\text{th}}$ natural mode of nonrotating blade             |
| $\omega$                 | natural frequency of blade vibration   |
| $\Omega$                 | rotational velocity  |

Subscripts:

|    |                       |
|----|-----------------------|
| R  | rotating              |
| NR | nonrotating           |
| n  | order of natural mode |
| o  | value at $x = 0$      |
| T  | value at $x = R$      |

Primes denote differentiation with respect to  $x$ .

THE RAYLEIGH-SOUTHWELL APPROXIMATION

In a free vibration of an elastic beam at one of its natural frequencies, the kinetic energy of the beam at zero displacement is equal to its potential energy at maximum displacement. When the beam is rotating, the potential energy includes a part associated with the centrifugal force field, in addition to the strain energy.

Considering displacements both normal to and in the plane of rotation, the kinetic energy may be written

$$\text{K.E.} = \frac{1}{2} \omega_{R_n}^2 \int_0^R \rho (\delta_{y_n}^2 + \delta_{z_n}^2) dx \quad , \quad (1)$$

where n refers to the mode under consideration.

Similarly, the potential energy may be written,

$$\begin{aligned} \text{P.E.} = & \frac{1}{2} \int_0^R \left\{ EI_1 (\delta_{y_n}'' \sin \beta + \delta_{z_n}'' \cos \beta)^2 + \right. \\ & \left. EI_2 (\delta_{y_n}'' \cos \beta + \delta_{z_n}'' \sin \beta)^2 \right\} dx + \\ & \frac{1}{2} \Omega^2 \int_0^R \left\{ T_1 (\delta_{y_n}'^2 + \delta_{z_n}'^2) - \rho \delta_{y_n}^2 \right\} dx \quad , \quad (2) \end{aligned}$$

where the first term is the strain energy and the second term is associated with the centrifugal force field.

Equating Eqs. (1) and (2) and solving for  $\omega_{R_n}^2$  yields

$$\omega_{R_n}^2 = \frac{\int_0^R \left\{ EI_1 (\delta_{y_n}'' \sin \beta + \delta_{z_n}'' \cos \beta)^2 + EI_2 (\delta_{y_n}'' \cos \beta + \delta_{z_n}'' \sin \beta)^2 \right\} dx}{\int_0^R \rho (\delta_{y_n}^2 + \delta_{z_n}^2) dx} + \frac{\int_0^R \left\{ T_1 (\delta_{y_n}'^2 + \delta_{z_n}'^2) - \rho \delta_{y_n}^2 \right\} dx}{\int_0^R \rho (\delta_{y_n}^2 + \delta_{z_n}^2) dx} \quad . \quad (3)$$

Equation (3) is correct only when  $\delta_{y_n}$  and  $\delta_{z_n}$  represent the true mode shape for the rotating beam, which is in general not known initially. It will, however, provide an approximate value of the frequency if a mode shape is used which resembles the true mode shape. If, as in the case of the untwisted beam, the rotation of the beam does not greatly change its natural mode shapes, it can be expected that Eq. (3) will yield a satisfactory approximate value for  $\omega_{R_n}$  when the corresponding mode shape,  $\phi_{y_n}$ ,  $\phi_{z_n}$ , for the nonrotating beam is used. When that is done, the first term on the right-hand side becomes the corresponding natural frequency of the nonrotating beam, and the equation may be written

$$\omega_{R_n}^2 = \omega_{NR_n}^2 + K_n \Omega^2, \quad (4)$$

where

$$K_n = \frac{\int_0^R \{T_1 (\phi_{y_n}'^2 + \phi_{z_n}'^2) - \rho \phi_{y_n}^2\} dx}{\int_0^R \rho (\phi_{y_n}^2 + \phi_{z_n}^2) dx}, \quad (5)$$

and is seen to depend only on the mass distribution of the beam and the shape of the  $n^{\text{th}}$  natural mode when  $\Omega = 0$ . It is referred to as the Southwell coefficient.

#### PROGRAM OF INVESTIGATION

A program of computations was performed for selected values of the significant parameters, using the method of the Appendix with the blade divided into ten equal segments. The error in frequency introduced by this approximate representation when the blade is nonrotating was found to be positive and was estimated to be about 1.5% in the case of the highest modes considered and to decrease accordingly for the lower modes. There is evidence, as discussed in the following section, that there is a further error introduced in the rotational case, which is negative and which consequently tends to reduce the ratio of the higher frequencies to their nonrotational values. These errors, while not insignificant in themselves, should not be substantially influenced by twist, and consequently would not be expected to mask the effect of twist on the natural frequencies.

As discussed in the Introduction, two types of mass and stiffness distribution were considered, namely, uniform distribution and linear taper to zero at the tip. The latter distribution was considered only in the case of zero rotational velocity. In addition, three values of  $\gamma$ —0, 0.1 and  $\sqrt{0.1}$ —were considered. The blades were assumed to be twisted linearly, the total angle of twist  $\theta$ , measured from the axis of rotation to the blade tip, being given values of  $0^\circ$ ,  $15^\circ$  and  $30^\circ$ . For each of these values of twist angle, three different blade angular settings were considered, involving  $\beta$  values at the tip of  $0^\circ$ ,



15° and 30°. Two different types of root support, namely, cantilever and fully articulated, were considered, the location of this support being either at the axis of rotation ( $\bar{e} = 0$ ) or offset from it by an amount equal to 5% of the rotor radius ( $\bar{e} = 0.05$ ).

The rotational velocity parameter,  $\mu$ , was varied from 0 to 15, with the bulk of the computations performed at values of 0, 10, and 15. This range is believed to include most practical cases. Mode shapes were determined in the cases of zero rotation and this information was used in testing the Rayleigh-Southwell approximation for the effect of rotational velocity.

Another approximation considered was that given by the following relation due to Lo and Renbarger, for the effect of blade angle on the natural frequencies of an untwisted rotating blade with  $\gamma = 0.10$

$$\omega_{R\beta}^2 = \omega_{R\beta=0}^2 - \Omega^2 \sin^2 \beta \quad (6)$$

This relation, which is exact for linearized vibration theory for untwisted blades, was tested for applicability as an approximation in the determination of the fundamental frequency of a twisted, rotating, cantilever blade, using the blade angle at the root.

## DISCUSSION OF RESULTS

### The Nonrotating Twisted Blade

The influence of twist and of the parameter  $\gamma$  on the natural frequencies of a nonrotating blade is shown in Figs. 4 to 7 inclusive. It is seen that the fundamental frequency is almost completely unaffected by these two parameters in every case considered. There is actually a very slight increase in frequency with increase in twist, but it is not discernible on the graphs. The effect of  $\gamma$  can also be expected to remain slight as long as  $\gamma$  is not close to 1.

Figures 4 and 5 illustrate the effect of  $\gamma$  on the higher frequencies considered. On these plots the bending stiffness  $EI_1$  remains constant as  $\gamma$  is varied; that is, only the stiffness  $EI_2$  is varied. This occurs directly as a result of the nondimensionalization of  $\omega$  in terms of  $EI_{10}$ .

For  $\gamma = 0$ , that is, for the blade infinitely stiff about the minor principal axis, it is seen that the higher modes reduce in frequency as the twist is increased. As  $\gamma$  is increased, an additional spectrum of frequencies moves to the left, which, for zero twist, corresponds to modes in bending about the minor principal axis of the cross section (chordwise bending). It is seen that, whenever one of these frequencies is close in value to a frequency in the original set for bending about the major principal axis (flapwise bending), twist has a strong coupling effect and tends to drive the two frequencies apart.

Figures 6 and 7 show the same frequency variations on a percentage basis. It should be noted that some of the frequency ratios correspond to modes which, for zero twist, involve displacement in the direction of the major principal axis of the cross section. It is seen that, for the most part, the effect of twist is substantially reduced with the introduction of taper in mass and stiffness.

### The Rotating Twisted Blade

Figure 8 demonstrates the combined effect of twist and rotational velocity on the absolute values of the natural frequencies for different values of  $\gamma$  for the case of the cantilever beam. It is seen that, when  $\gamma = 0$ , the frequencies are all well separated and the trends introduced by twist at zero rotational velocity are maintained as rotational velocity is increased, except that the effect of twist on the frequency of the fundamental mode becomes quite pronounced at the higher values of  $\mu$  if the tip blade angle is maintained constant.

This situation is altered considerably as  $\gamma$  is increased because of important coupling effects introduced by twist. It is seen that for zero twist and zero blade angle the effect of rotation on the frequencies for flapwise bending is much greater than that on the frequencies for chordwise bending. As a consequence, frequency curves for flapwise and chordwise bending may cross, and this is indeed seen to be what happens for both  $\gamma^2 = 0.01$  and  $\gamma^2 = 0.1$ , two such intersections occurring in the latter case. However, when twist is introduced, the intersections are seen no longer to occur. This must be attributed to a strong influence of twist in coupling the flapwise and chordwise motions, and it must be concluded that, due to this coupling, the character of the individual modes changes substantially but continuously as the rotational velocity is increased from zero to large values.

Presentation of the frequency data in the manner of Fig. 8, while valuable in demonstrating the effects just discussed, does not lend itself well to a generalization of the data in a useful form. For this purpose it is preferable to express the natural frequencies of the rotating blade in the form of a ratio to the corresponding frequencies of the nonrotating blade and the rotational velocity in the form of a ratio to the fundamental frequency of the nonrotating blade. This is done in Figs. 9 to 13 inclusive, which contain all the data generated. These figures demonstrate the effect of tip blade angle,  $\beta_T$ , for given values of total twist. In most cases data are presented for both zero and 5% offset and for both cantilever- and articulated-type root support. It is seen that, while the effect of blade angle is large in the case of the fundamental frequency ratio, its effect decreases rapidly as the order of the frequency is increased, and, for many of the higher frequencies, is negligible. It appears also that twist tends to reduce the blade-angle effect on the higher frequencies.

It should be noted that the discontinuity in slope of some of the curves for zero twist, as, for instance, in Fig. 10a, is attributable to the fact that the curves are plotted for modes of given order, and when a discontinuity occurs, the mode of given order changes abruptly from a chordwise to a flapwise mode, or

vice versa, as seen in Fig. 8. Since no abrupt change occurs in the character of a mode with increase in rotational velocity when the blade is twisted, as seen in Fig. 8, the curves for the twisted blades are smooth. The same is apparently true when there is zero twist but the blade angle is different from zero, as seen in Fig. 11a, since blade angle in the rotational case also has the effect of coupling bending vibrations in the directions of the two principal axes of the cross section. In the case of the higher modes, this effect appears to be small at moderate values of the blade angle, as seen in Fig. 10a.

The effect of offset of the root support is seen to follow the trend disclosed in Ref. 1 for untwisted blades; that is, the centrifugal force has an increased stiffening effect and consequently increases the frequency ratio. In view of the conclusion reached in Ref. 11, that the frequencies depend almost linearly on the amount of offset in the case of an untwisted beam at given rotational velocity, it appears safe to extend this conclusion to twisted beams with moderate offset, and to determine frequencies for amounts of offset other than those specified here by linear interpolation or extrapolation from the present data.

Figures 9 to 13 are not convenient for an evaluation of the effect of twist. For this purpose the plots of Figs. 14 to 18 inclusive are considerably more advantageous. Figure 14 shows that, for  $\gamma = 0$ , the fundamental frequency of the uniform cantilever beam is highly dependent on twist when the blade angle at the tip is maintained constant and only slightly dependent on twist when the blade angle at the root is maintained constant. This indicates that in this case the dependence is primarily on root blade angle rather than twist. Furthermore, the reversal in the trend of the curves with twist variation when the tip and root angles are maintained constant, indicates that there is an intermediate station, not far from the root, such that, if the blade angle is maintained constant at that station, the fundamental frequency will be independent of twist. It can be anticipated that its location in the general case will be dependent upon the mass and stiffness distribution of the blade, and that it will tend to move outward with increasing taper in stiffness.

In the case of the higher modes, it is seen that twist has a negligible effect on frequency, irrespective of where the blade angle is maintained constant. In view of this conclusion and the corresponding small effect of blade angle, discussed earlier, it appears that the frequency ratios for these modes when the blade is very stiff in chordwise bending relative to flapwise bending ( $\gamma \ll 0.1$ ) can be estimated satisfactorily by neglecting blade angle and twist. For this purpose the data of Ref. 1 could be used. It would, of course, be necessary to determine the natural frequencies of the nonrotating twisted blade to convert frequency ratios into actual frequencies. For this purpose, methods such as those of the Appendix or Ref. 12 could be used.

Figure 15 indicates that, when  $\gamma^2 = 0.01$ , conclusions similar to those discussed above with regard to the fundamental frequency of the uniform cantilever blade when  $\gamma = 0$  apply again. In the case of those higher frequencies which

evidence substantial coupling effects, there is now a moderate influence of twist on the frequency ratio.

When  $\gamma^2$  is increased further to the value 0.1, there is substantial coupling between the fundamental flapwise and chordwise modes, but it is still seen (Fig. 16) that the frequency ratios for these modes are primarily functions of root angle and are only slightly dependent on twist. In the case of the higher modes, coupling is again seen to effect a moderate dependence of frequency ratio on twist.

In the case of the uniform articulated blade, the relative absence of coupling effects for the parametric values and modes considered produces results similar to those discussed above in connection with the cantilever blade with  $\gamma = 0$ . The fundamental frequency ratio is again independent of twist if the blade angle is maintained constant at an intermediate station, which in this case can be expected to be considerably further out along the blade. The frequency ratio for the second mode is seen to be virtually independent of both twist and blade angle for moderate values of the twist and blade angle.

#### Evaluation of the Rayleigh-Southwell Approximation

The Rayleigh-Southwell approximation was applied to most of the zero-offset cases considered and the results are shown in Figs. 9 to 13 inclusive. It is seen from Fig. 9 that, with  $\gamma^2 = 0$ , the error introduced by the approximation into the fundamental frequency of the uniform cantilever blade increases substantially with twist and with blade angle in the range considered. On the other hand, these parameters are seen to have little effect on the accuracy of the approximation in the case of the higher frequencies.

It should be noted that the results for zero twist and blade angle indicate a discrepancy with corresponding results in Ref. 1 for the higher frequencies, the error introduced by the Rayleigh-Southwell approximation being different both in magnitude and sign. This indicates that the method of the Appendix yields values for the higher frequencies of a rotating blade which are lower relative to the corresponding frequencies of the nonrotating blade than they would be in an exact determination. It is not expected, however, that this error is sufficiently affected by blade angle or twist to alter any conclusions reached with regard to the effect of these parameters on the accuracy of the Rayleigh-Southwell approximation.

Figures 10 and 11 indicate that, as  $\gamma$  is increased, conclusions similar to those reached above for  $\gamma^2 = 0$  still apply in the case of frequencies which are not substantially influenced by coupling between bending about the two principal axes of the cross section. On the other hand, where such coupling is large, the curves of frequency ratio depart radically from a straight-line variation and the Rayleigh-Southwell approximation loses its value, except at low values of the rotational velocity. This could easily be anticipated, since the mode

shapes, in such cases, can be expected to change radically with increase in the rotational velocity.

In the case of the articulated blade (Figs. 12 and 13), no strong coupling effects, as discussed above, were encountered for the parametric values considered. Consequently, the Rayleigh-Southwell approach was found to yield a valid approximation in these cases. The error introduced by it is seen to be relatively insensitive to twist, but to decrease somewhat with increase in blade angle.

#### Evaluation of the Relation of $L_0$ and Renbarger in Application to Twisted Blades

The applicability of Eq. (6) in the determination of the fundamental frequency of a rotating, uniform, twisted, cantilever blade, using the blade angle at the root, is illustrated in Fig. 19. It is seen that the accuracy of this relation deteriorates somewhat with increase in twist, but it still represents a valid approximation for estimation purposes. It is seen also that the slope of the actual curves is very close to that of the approximation. Results are not presented for  $\gamma^2 = 0.1$ , since the large coupling effects present in that case would be expected to make Eq. (6) inapplicable.

#### CONCLUDING REMARKS

On the basis of the data presented, a number of conclusions can be reached concerning the natural frequencies of twisted nonrotating and rotating blades. These are:

- (1) The fundamental frequency of cantilever and articulated nonrotating blades is effectively independent of twist if the bending stiffness about the minor principal axis of the cross section is at least three times as large as the bending stiffness about the major principal axis.
- (2) The second and third natural frequencies of nonrotating cantilever blades and the second natural frequency of nonrotating articulated blades decrease with increase in twist if the stiffness about the minor principal axis of the cross section is very large in relation to the stiffness about the major principal axis.
- (3) When two frequencies of a nonrotating untwisted blade are close to each other in value, the introduction of twist tends to increase the separation of the two frequency values.
- (4) The effect of twist on the lower natural frequencies of nonrotating blades decreases with increase in taper of both mass and stiffness.

(5) The fundamental frequency of a rotating twisted cantilever blade depends primarily on root blade angle and only secondarily on twist. It is independent of twist when the blade angle is maintained constant at an appropriately selected intermediate station close to the root. The location of this station can be expected to depend upon the spanwise distribution of mass and stiffness. A similar station exists in the case of the fundamental frequency of a rotating twisted articulated blade, but it is located considerably further outboard.

(6) When curves of natural frequency versus rotational velocity for an untwisted blade set at zero-blade-angle cross, the introduction of twist or blade angle tends to couple the corresponding modes and yields frequency curves which do not cross.

(7) When coupling effects, as discussed in Item 6, are not appreciable, the effect of twist and blade angle on the ratio of rotating to nonrotating frequencies of the higher modes is small or negligible. Even when such coupling effects are large, the frequency ratio is not highly sensitive to blade angle or twist.

(8) Offset of the root support increases the frequency ratio.

(9) The Rayleigh-Southwell approximation yields results, in the case of twisted rotating blades, which are similar to those of the untwisted blade at zero blade angle<sup>1</sup> for the higher modes when coupling effects of the sort discussed in Item (6) are not in evidence. When such coupling effects are in evidence, the approach yields very poor results except at small values of rotational velocity. The fundamental frequency of a cantilever blade is less well represented by the Rayleigh-Southwell approximation when twist and blade angle are introduced. On the other hand, the accuracy of the approximation in determining the fundamental frequency of an articulated blade is relatively insensitive to twist and improves with increase in the blade angle.

(10) The relation of Lo and Renbarger for the effect of blade angle on natural frequency of rotating blades is found to be useful in determining the fundamental frequency of twisted cantilever blades when blade angle is measured at the root of the blade and the fundamental mode is not substantially coupled with other modes.

## APPENDIX

### METHOD OF ANALYSIS

The present method of analysis represents a modification of a method developed by Targoff,<sup>8</sup> which in turn is an extension and adaptation of the familiar Holzer-Myklestad method<sup>9</sup> to the case of bending of a twisted rotating beam.

The beam is divided spanwise into a number of segments, not necessarily equal in length. The mass of each segment is assumed concentrated at its center, and the bending stiffnesses  $EI_1$  and  $EI_2$  and angle of incidence  $\beta$  are assumed constant between masses, appropriate average values being selected. The twist of the beam is accounted for by relative rotations of adjacent uniform bays (between masses) about a spanwise axis, the change in angle,  $\Delta\beta$ , being equal to the total twist in a segment and occurring just outboard of the mass, as shown in Fig. 1.

The quantities  $V_1, M_1, \delta_1', \delta_1, V_2, M_2, \delta_2'$  and  $\delta_2$  (Fig. 3), applying when the beam is at its maximum displacement in a free vibration, are defined at stations along the beam, and may be represented, at any station, in the form of a column matrix,

$$\{\Delta\} = \begin{Bmatrix} V_1 \\ M_1 \\ \delta_1' \\ \delta_1 \\ V_2 \\ M_2 \\ \delta_2' \\ \delta_2 \end{Bmatrix} .$$

The elements of this matrix will vary as one moves along the beam, and in such a manner that the variation can be considered to occur in a series of steps. Moving from the tip towards the root of the beam, the change in  $\{\Delta\}$  occurring from a station immediately outboard of one mass to a station immediately outboard of the next mass can be broken down into three steps, the first involving movement across the mass, the second involving movement from one end to the other of the weightless uniform bay, and the third involving movement across the discontinuity in  $\beta$ .

The relationship between the  $\{\Delta\}$  matrices as they apply at the two extremes of this travel can be represented as follows:

$$\{\Delta\}_{n+1} = [R] [E] [F] \{\Delta\}_n , \quad (A1)$$

where [F], [E], and [R] are rectangular matrices representing linear relationships corresponding to the three steps discussed above.

The [F] matrix, relating the  $\{\Delta\}$  matrices on either side of a concentrated mass, is written as follows:

$$[F] = \begin{bmatrix} 1 & 0 & 0 & m(\omega^2 + \Omega^2 \sin^2\beta) & 0 & 0 & 0 & -m\Omega^2 \sin\beta \cos\beta \\ 0 & 1 & 0 & -m\Omega^2 x & 0 & 0 & 0 & 0 \\ 0 & 0 & 1 & 0 & 0 & 0 & 0 & 0 \\ 0 & 0 & 0 & 1 & 0 & 0 & 0 & 0 \\ 0 & 0 & 0 & -m\Omega^2 \sin\beta \cos\beta & 1 & 0 & 0 & m(\omega^2 + \Omega^2 \cos^2\beta) \\ 0 & 0 & 0 & 0 & 0 & 1 & 0 & -m\Omega^2 x \\ 0 & 0 & 0 & 0 & 0 & 0 & 1 & 0 \\ 0 & 0 & 0 & 0 & 0 & 0 & 0 & 1 \end{bmatrix} \quad (A2)$$

It is seen that only the shear forces and bending moments are changed, since there are no discontinuities in slope or displacement. The changes in shear force are due partly to the inertia force associated with the vibrational motion of the mass and partly to the component of centrifugal force normal to the undeformed position of the elastic axis. The change in bending moment is fictitious and arises from a special feature of the analysis. This feature involves the replacement of the component of the centrifugal force parallel to the undeformed position of the elastic axis by an equal force along the line of the undeformed axis and an appropriate couple to provide static equivalence. The changes in bending moment indicated in the [F] matrix are then due only to the applied couple, the moment due to the force applied along the undeformed axis being accounted for in the [E] matrix. When moments due to both sources are considered, the discontinuity in bending moment disappears. It should be noted that, on the basis of this procedure, the bending moment at any station is not  $M$ , but rather  $M$  plus the moment of the tensile force  $T$  acting along the undeformed elastic axis.

The elements in the [E] matrix are found by solution of the differential equation for bending in the weightless uniform bay between masses. For bending about the major principal axis of the cross section, this equation is written as follows:

$$\delta_1'' EI_1 = V_1 s + (M_1 + T \delta_1) , \quad (A3)$$

where  $V_1$  and  $M_1$  apply at the outboard end of the bay, and  $s$  is a spanwise coordinate measured inward from the outer end of the bay.



The solution of Eq. (A3) is

$$\delta_1(s) = \delta_1(0) \cosh(p_1 s) + \delta_1'(0) \frac{\sinh(p_1 s)}{p_1} + \frac{M_1}{T} \{ \cosh(p_1 s) - 1 \} + \frac{V_1}{T} \left\{ \frac{1}{p_1} \sinh(p_1 s) - s \right\}, \quad (A4)$$

where

$$p_1 = \sqrt{\frac{T}{EI_1}}.$$

Substituting  $s = l$ , where  $l$  is the length of the bay, into this solution and its first derivative and into a similar solution for bending about the minor principal axis of the cross section, the elements of the [E] matrix are obtained. This matrix is presented as follows:

[E] =

$$\begin{bmatrix} 1 & 0 & 0 & 0 & 0 & 0 & 0 & 0 \\ l & 1 & 0 & 0 & 0 & 0 & 0 & 0 \\ E_{31} & E_{32} & E_{33} & E_{34} & 0 & 0 & 0 & 0 \\ E_{41} & E_{42} & E_{43} & E_{44} & 0 & 0 & 0 & 0 \\ 0 & 0 & 0 & 0 & 1 & 0 & 0 & 0 \\ 0 & 0 & 0 & 0 & l & 1 & 0 & 0 \\ 0 & 0 & 0 & 0 & E_{75} & E_{76} & E_{77} & E_{78} \\ 0 & 0 & 0 & 0 & E_{85} & E_{86} & E_{87} & E_{88} \end{bmatrix}, \quad (A5)$$

where

$$E_{31} = -E_{42} = -\frac{1}{T} \{ \cosh(p_1 l) - 1 \}$$

$$E_{32} = -\frac{p_1}{T} \sinh(p_1 l)$$

$$E_{33} = E_{44} = \cosh(p_1 l)$$

$$E_{34} = -p_1 \sinh(p_1 l)$$

$$E_{41} = \frac{1}{T} \left\{ \frac{1}{p_1} \sinh(p_1 l) - l \right\}$$

$$E_{43} = -\frac{1}{p_1} \sinh(p_1 l)$$

$$E_{75} = -E_{86} = -\frac{1}{T} \{ \cosh(p_2 l) - 1 \}$$

$$E_{76} = -\frac{p_2}{T} \sinh(p_2 l)$$

$$E_{77} = E_{88} = \cosh(p_2 l)$$

$$E_{78} = -p_2 \sinh(p_2 l)$$

$$E_{85} = \frac{1}{T} \left\{ \frac{1}{p_2} \sinh(p_2 l) - l \right\}$$

$$E_{87} = -\frac{1}{p_2} \sinh(p_2 l) \quad .$$

It should be noted that  $\delta_1'$  and  $\delta_2'$  are positive for increasing deflection in the positive direction of  $x$ .

The  $[R]$  matrix serves merely to rotate the coordinate axes through the angle  $\Delta\beta$ , and is written as follows:

$[R] =$

$$\begin{bmatrix} \cos \Delta\beta & 0 & 0 & 0 & -\sin \Delta\beta & 0 & 0 & 0 \\ 0 & \cos \Delta\beta & 0 & 0 & 0 & -\sin \Delta\beta & 0 & 0 \\ 0 & 0 & \cos \Delta\beta & 0 & 0 & 0 & -\sin \Delta\beta & 0 \\ 0 & 0 & 0 & \cos \Delta\beta & 0 & 0 & 0 & -\sin \Delta\beta \\ \sin \Delta\beta & 0 & 0 & 0 & \cos \Delta\beta & 0 & 0 & 0 \\ 0 & \sin \Delta\beta & 0 & 0 & 0 & \cos \Delta\beta & 0 & 0 \\ 0 & 0 & \sin \Delta\beta & 0 & 0 & 0 & \cos \Delta\beta & 0 \\ 0 & 0 & 0 & \sin \Delta\beta & 0 & 0 & 0 & \cos \Delta\beta \end{bmatrix}$$

By a successive multiplication of the appropriate matrices, a linear relationship can be established between the  $\{\Delta\}$  matrices at the root and tip of the beam.

$$\{\Delta\}_{\text{root}} = [C]\{\Delta\}_{\text{tip}} \quad (A6)$$

Recognizing that the shears and bending moments are zero at the tip of the beam, the  $\{\Delta\}_{\text{tip}}$  matrix can be reduced to a four-element matrix and the corresponding four columns of the  $[C]$  matrix eliminated. In fact, these four columns can be eliminated from the first  $[F]$  matrix at the tip of the beam, and successive multiplications will then yield an  $8 \times 4$  matrix product.

Satisfaction of the boundary conditions at the root of the beam then requires that the determinant of a  $4 \times 4$  matrix formed from appropriate elements of the  $[C]$  matrix be equal to zero. The elements of this determinant will be polynomials in  $\omega^2$ , and, upon expansion, a polynomial equation in  $\omega^2$  will be obtained. In principle, the natural frequencies of the beam could be determined by solving for the roots of this equation. Such a procedure would be far too cumbersome to be feasible, however.

A more practical procedure involves the introduction of trial values of  $\omega$  into the various  $[F]$  matrices and evaluating the elements of all the matrices numerically. The matrix multiplications can then be carried out numerically and the appropriate determinant evaluated. The value of this determinant, which may be termed the "residual," may then be plotted versus  $\omega$  or  $\omega^2$ , and the location of zeros of the residual will determine the natural frequencies of the beam.

For the purposes of a parametric survey, it is desirable to treat the problem in nondimensional form. Toward this end, the  $\{\Delta\}$  matrix can be redefined in terms of nondimensional forces and moments as follows:

$$\{\Delta\} = \begin{Bmatrix} V_1 R^2 / EI_{10} \\ M_1 R / EI_{10} \\ \delta_1' \\ \delta_1 / R \\ V_2 R^2 / EI_{10} \\ M_2 R / EI_{10} \\ \delta_2' \\ \delta_2 / R \end{Bmatrix} \quad (A7)$$

The corresponding nondimensional forms for the [F] and [E] matrices are as follows, the [R] matrix remaining unchanged:

$$[F] = \begin{bmatrix} 1 & 0 & 0 & \bar{l} \bar{\rho} (\lambda^2 + \mu^2 \sin^2 \beta) & 0 & 0 & 0 & -\bar{l} \bar{\rho} \mu^2 \sin \beta \cos \beta \\ 0 & 1 & 0 & -\bar{l} \bar{\rho} \bar{x} \mu^2 & 0 & 0 & 0 & 0 \\ 0 & 0 & 1 & 0 & 0 & 0 & 0 & 0 \\ 0 & 0 & 0 & 1 & 0 & 0 & 0 & 0 \\ 0 & 0 & 0 & -\bar{l} \bar{\rho} \mu^2 \sin \beta \cos \beta & 1 & 0 & 0 & \bar{l} \bar{\rho} (\lambda^2 + \mu^2 \cos^2 \beta) \\ 0 & 0 & 0 & 0 & 0 & 1 & 0 & -\bar{l} \bar{\rho} \bar{x} \mu^2 \\ 0 & 0 & 0 & 0 & 0 & 0 & 1 & 0 \\ 0 & 0 & 0 & 0 & 0 & 0 & 0 & 1 \end{bmatrix}, (A8)$$

$$[E] = \begin{bmatrix} 1 & 0 & 0 & 0 & 0 & 0 & 0 & 0 \\ \bar{l} & 1 & 0 & 0 & 0 & 0 & 0 & 0 \\ \bar{E}_{31} & \bar{E}_{32} & \bar{E}_{33} & \bar{E}_{34} & 0 & 0 & 0 & 0 \\ \bar{E}_{41} & \bar{E}_{42} & \bar{E}_{43} & \bar{E}_{44} & 0 & 0 & 0 & 0 \\ 0 & 0 & 0 & 0 & 1 & 0 & 0 & 0 \\ 0 & 0 & 0 & 0 & \bar{l} & 1 & 0 & 0 \\ 0 & 0 & 0 & 0 & \bar{E}_{75} & \bar{E}_{76} & \bar{E}_{77} & \bar{E}_{78} \\ 0 & 0 & 0 & 0 & \bar{E}_{85} & \bar{E}_{86} & \bar{E}_{87} & \bar{E}_{88} \end{bmatrix}, (A9)$$

where

$$\begin{aligned} \bar{E}_{31} &= -\bar{E}_{42} = -\frac{1}{\mu^2 \bar{T}} \left\{ \cosh \mu \left( \bar{l} \sqrt{\frac{\bar{T}}{EI_1}} \right) - 1 \right\} \\ \bar{E}_{32} &= -\frac{1}{\mu \sqrt{\bar{T} EI_1}} \sinh \left( \mu \bar{l} \sqrt{\frac{\bar{T}}{EI_1}} \right) \\ \bar{E}_{33} &= \bar{E}_{44} = \cosh \left( \mu \bar{l} \sqrt{\frac{\bar{T}}{EI_1}} \right) \\ \bar{E}_{34} &= -\mu \sqrt{\frac{\bar{T}}{EI_1}} \sinh \left( \mu \bar{l} \sqrt{\frac{\bar{T}}{EI_1}} \right) \end{aligned}$$

$$\begin{aligned}
\bar{E}_{41} &= \frac{1}{\mu^2 \bar{T}} \left\{ \frac{1}{\mu} \sqrt{\frac{\bar{E}I_1}{\bar{T}}} \sinh \left( \mu \bar{l} \sqrt{\frac{\bar{T}}{\bar{E}I_1}} \right) - \bar{l} \right\} \\
\bar{E}_{43} &= -\frac{1}{\mu} \sqrt{\frac{\bar{E}I_1}{\bar{T}}} \sinh \left( \mu \bar{l} \sqrt{\frac{\bar{T}}{\bar{E}I_1}} \right) \\
\bar{E}_{75} &= -\bar{E}_{86} = -\frac{1}{\mu^2 \bar{T}} \left\{ \cosh \left( \gamma \mu \bar{l} \sqrt{\frac{\bar{T}}{\bar{E}I_2}} \right) - 1 \right\} \\
\bar{E}_{76} &= -\frac{\gamma}{\mu \sqrt{\bar{T} \bar{E}I_2}} \sinh \left( \gamma \mu \bar{l} \sqrt{\frac{\bar{T}}{\bar{E}I_2}} \right) \\
\bar{E}_{77} &= \bar{E}_{88} = \cosh \left( \gamma \mu \bar{l} \sqrt{\frac{\bar{T}}{\bar{E}I_2}} \right) \\
\bar{E}_{78} &= -\mu \gamma \sqrt{\frac{\bar{T}}{\bar{E}I_2}} \sinh \left( \gamma \mu \bar{l} \sqrt{\frac{\bar{T}}{\bar{E}I_2}} \right) \\
\bar{E}_{85} &= \frac{1}{\mu^2 \bar{T}} \left\{ \frac{1}{\mu \gamma} \sqrt{\frac{\bar{E}I_2}{\bar{T}}} \sinh \left( \gamma \mu \bar{l} \sqrt{\frac{\bar{T}}{\bar{E}I_2}} \right) - \bar{l} \right\} \\
\bar{E}_{87} &= -\frac{1}{\mu \gamma} \sqrt{\frac{\bar{E}I_2}{\bar{T}}} \sinh \left( \gamma \mu \bar{l} \sqrt{\frac{\bar{T}}{\bar{E}I_2}} \right) .
\end{aligned}$$

For the case of zero rotational velocity, the [F] matrix is obtained directly by substitution of  $\mu = 0$ . When this substitution is made in the [E] matrix, some of the elements are found to be of indeterminate form and a limiting process must be applied. This results in:

[E] =

$$\begin{bmatrix}
1 & 0 & 0 & 0 & 0 & 0 & 0 & 0 & 0 \\
\bar{l} & 1 & 0 & 0 & 0 & 0 & 0 & 0 & 0 \\
-\frac{\bar{l}^2}{2\bar{E}I_1} & -\frac{\bar{l}}{\bar{E}I_1} & 1 & 0 & 0 & 0 & 0 & 0 & 0 \\
\frac{\bar{l}^3}{6\bar{E}I_1} & \frac{\bar{l}^2}{2\bar{E}I_1} & -\bar{l} & 1 & 0 & 0 & 0 & 0 & 0 \\
0 & 0 & 0 & 0 & 1 & 0 & 0 & 0 & 0 \\
0 & 0 & 0 & 0 & \bar{l} & 1 & 0 & 0 & 0 \\
0 & 0 & 0 & 0 & -\frac{\gamma^2 \bar{l}^2}{2\bar{E}I_2} & -\frac{\gamma^2 \bar{l}}{\bar{E}I_2} & 1 & 0 & 0 \\
0 & 0 & 0 & 0 & \frac{\gamma^2 \bar{l}^3}{6\bar{E}I_2} & \frac{\gamma^2 \bar{l}^2}{2\bar{E}I_2} & -\bar{l} & 1 & 0
\end{bmatrix} . \quad (A10)$$

It has been found that a direct application of the method as indicated leads to computational difficulties under some circumstances. Roundoff errors in the succession of matrix multiplications and small differences between large numbers in the determinant expansion may result in considerable random error in the values of the residual, making it difficult to obtain an accurate estimate of the natural frequencies. Such errors are negligible when the rotational velocity is small and only the lower natural frequencies are desired. They increase with increase in the rotational velocity and the order of the desired natural frequencies, and may become very troublesome.

This difficulty can always be overcome by a sufficient increase in the number of significant figures carried in the computations, such as by the use of double-precision programming in machine computation, but only at the price of increased programming complexity, increased storage requirements, and greatly increased computing time. An alternative scheme for circumventing it has been devised by Targoff.<sup>13</sup> It involves a refinement of the basic method for values of frequency in the neighborhood of an expected solution. The basic method is applied at such a value, and three of the four unknown tip quantities (deflections and slopes) are related linearly to the fourth by solution of three of the four homogeneous equations obtained from Eq. (A6) for satisfaction of the root boundary conditions. This corresponds to an approximate mode shape. The correction to this approximation to yield the exact mode shape may then be represented as follows:

$$\begin{pmatrix} \delta_1' - \delta_{1a}' & \delta_1 \\ \delta_2' - \delta_{2a}' & \delta_1 \\ \delta_2' - \delta_{2a}' & \delta_2 \end{pmatrix},$$

where  $\delta_{1a}'$ ,  $\delta_{2a}'$ , and  $\delta_{2a}$  correspond to the approximate mode normalized for  $\delta_1 = 1$ . Thus, the following relation may be written:

$$\{\Delta\}_{tip} = \begin{bmatrix} 0 & 0 & 0 & 0 \\ 0 & 0 & 0 & 0 \\ 1 & \delta_{1a}' & 0 & 0 \\ 0 & 1 & 0 & 0 \\ 0 & 0 & 0 & 0 \\ 0 & 0 & 0 & 0 \\ 0 & \delta_{2a}' & 1 & 0 \\ 0 & \delta_{2a} & 0 & 1 \end{bmatrix} \begin{pmatrix} \delta_1' - \delta_{1a}' & \delta_1 \\ \delta_1 \\ \delta_2' - \delta_{2a}' & \delta_1 \\ \delta_2' - \delta_{2a}' & \delta_1 \end{pmatrix}. \quad (All)$$

If this relation is substituted into Eq. (A6) and the successive matrix multiplications are repeated, starting with the new  $8 \times 4$  matrix introduced by this substitution, it is found that the residuals determined in this manner show greatly reduced scatter and permit a more accurate determination of the natural frequencies. It should be noted that the present modification does not change the values of the frequency at which the zeros of the residual occur,

since it involves the addition to one column of the determinant of a linear combination of other columns, thus not changing the exact value of the determinant but merely scaling down one of its columns.

## REFERENCES

1. Yntema, R. T., Simplified Procedures and Charts for the Rapid Estimation of Bending Frequencies of Rotating Beams, NACA TN 3459, 1955.
2. Houbolt, J. C., and Brooks, G. W., Differential Equations of Motion for Combined Flapwise Bending, Chordwise Bending, and Torsion of Twisted Nonuniform Rotor Blades, NACA TN 3905, 1957.
3. Arnoldi, W. E., Response of a Rotating Propeller to Aerodynamic Excitation, NACA RM 8I07, 1949.
4. DeVries, J. A., and Stulen, F. B., A Complete Matrix Solution for the Vibratory Bending Moments of a Propeller Blade Subjected to a Pure First Order Aerodynamic Excitation, Rep. No. C-2152, Curtiss-Wright Corp., Propeller Div. (Caldwell, N. J.), May 16, 1950.
5. Niordson, F., "Vibrations of Rotating Twisted Beams," Tekniska Skrifter, Utgivna Av Svenska Teknologforeningen, Nr. 161, Stockholm, Sweden, 1957.
6. DiPrima, R. C., and Handelman, G. H., "Vibrations of Twisted Beams," Quart. J. Appl. Math., 12, 241-259 (October, 1954).
7. Boyce, W., and Handelman, G. H., Vibrations of Twisted Beams II, Rensselaer Polytechnic Institute, Math. Rep. No. 11, Dec. 19, 1957 (AFOSR TN-57-773).
8. Targoff, W., "The Bending Vibrations of a Twisted Rotating Beam," Proc. Third Midwestern Conf. on Solid Mechanics, Univ. of Mich. Press, Ann Arbor, Mich., 1957, pp. 177-194. (Also WADC Technical Report 56-27.)
9. Myklestad, N. O., Vibration Analysis, McGraw-Hill Book Co., New York, 1944.
10. Lo, H., and Renbarger, J. L., "Bending Vibrations of a Rotating Beam," Proc. First U. S. Nat. Cong. Appl. Mech. (Chicago, Ill., 1951), A.S.M.E., 1952, pp. 75-79.
11. Boyce, W. E., "Effect of Hub Radius on the Vibrations of a Uniform Bar," J. Appl. Mech., 23, 287 (June, 1956).
12. Mendelson, A., and Gendler, S., Analytical and Experimental Investigation of Effect of Twist on Vibrations of Cantilever Beams, NACA TN 2300, 1951.
13. Verbal communication from Mr. W. Targoff.

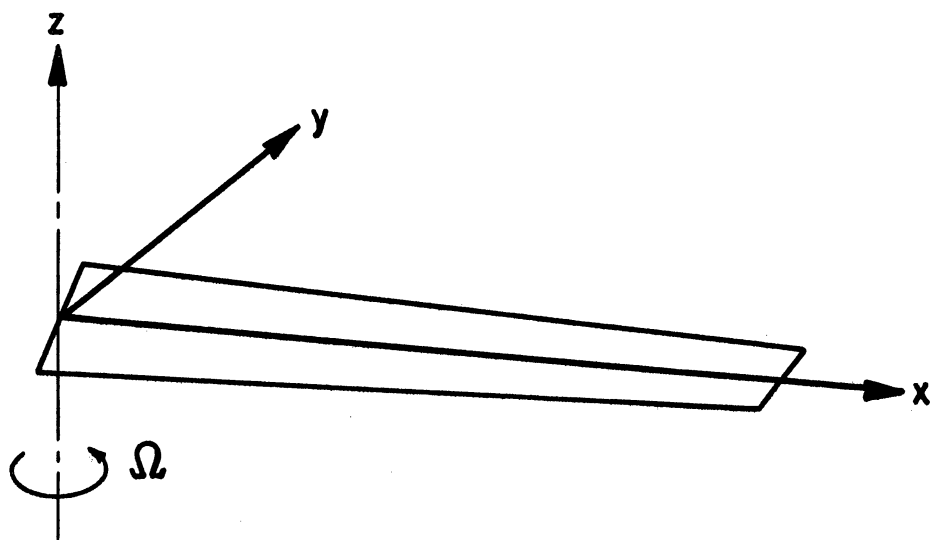
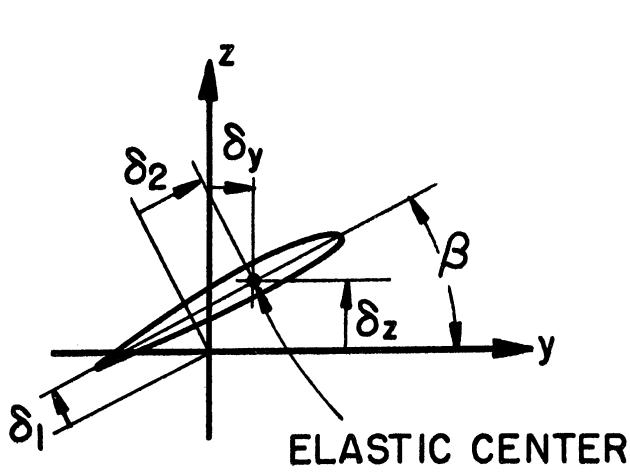
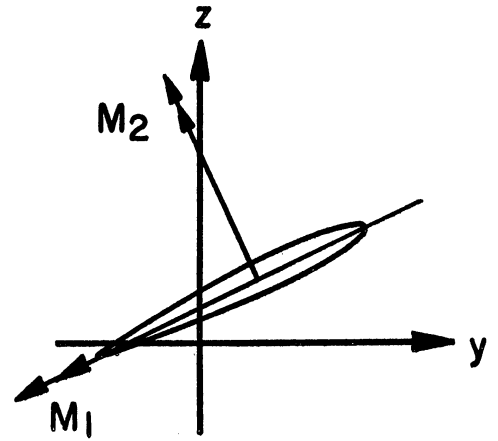


Fig. 1. Coordinate axes of blade.

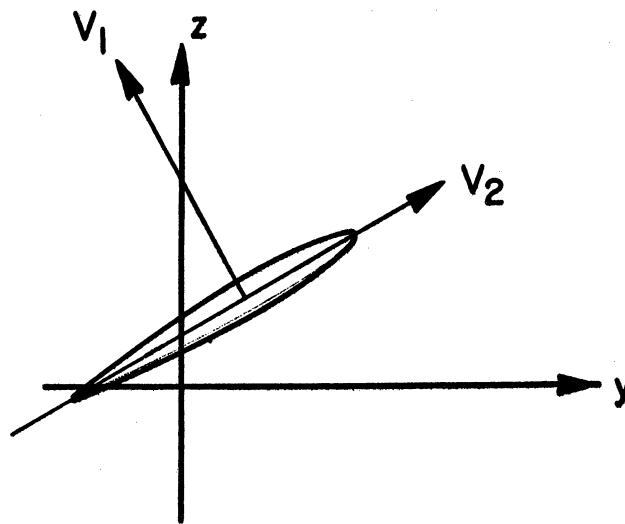




(a) DISPLACEMENTS



(b) MOMENTS



(c) SHEARS

Fig. 2. Nomenclature and sign convention for displacements, bending moments and shears (view of cross section looking toward axis of rotation).

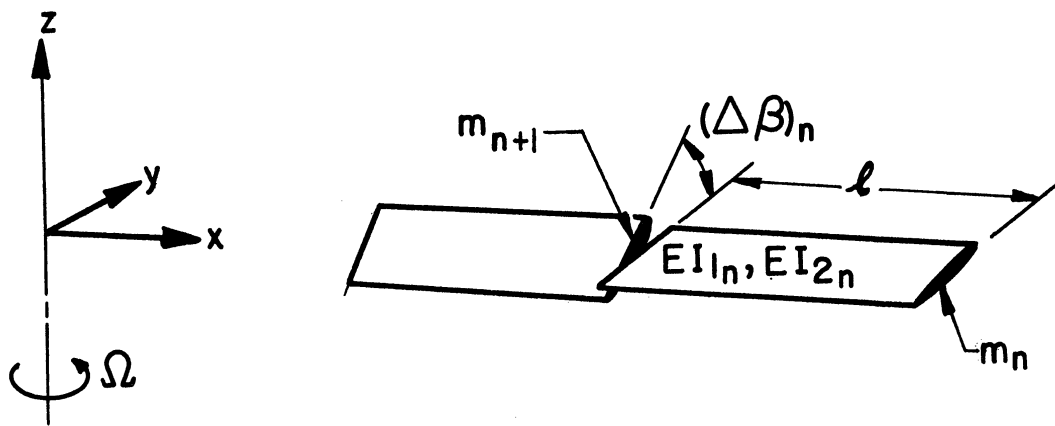


Fig. 3. Blade representation in method of Appendix.

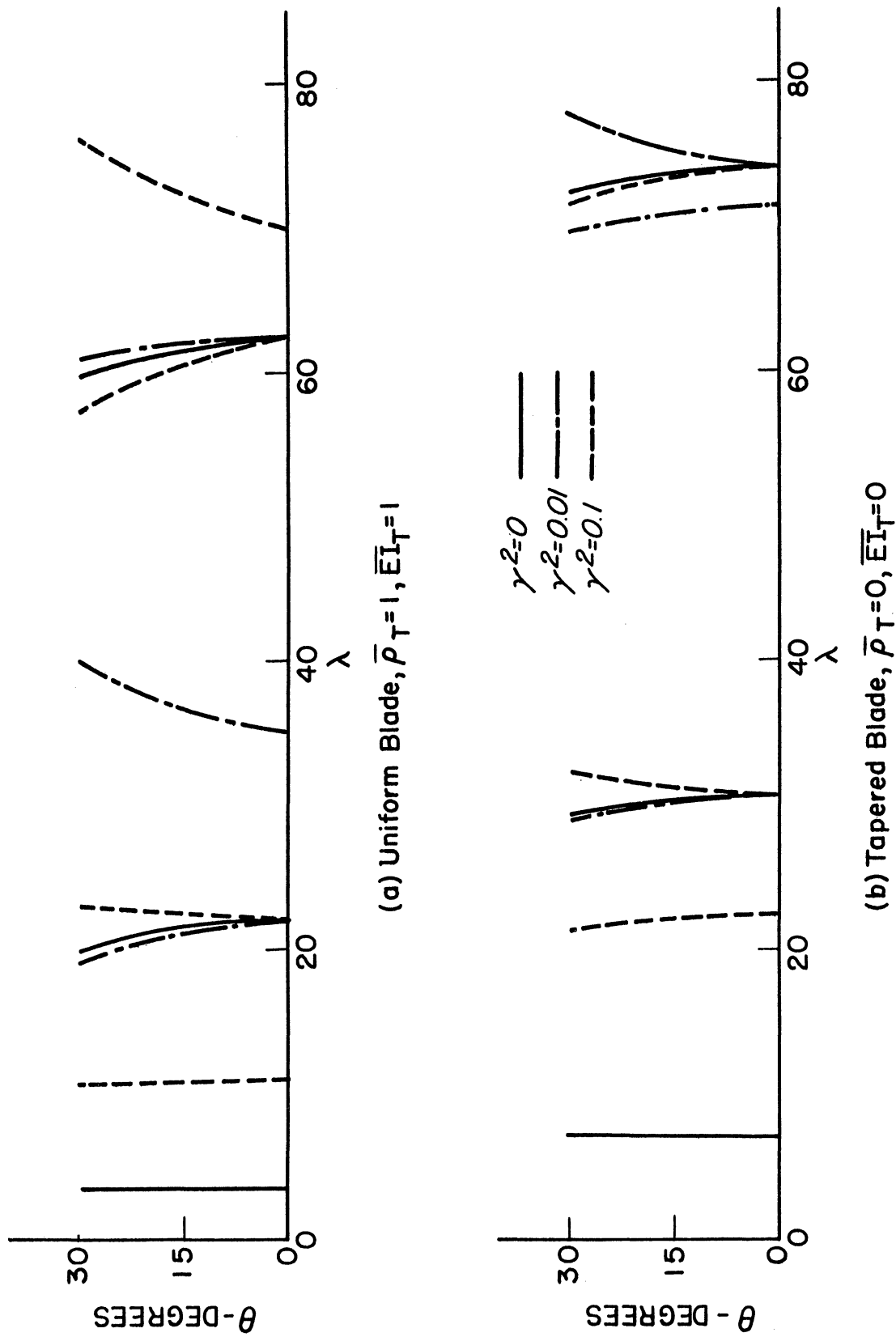
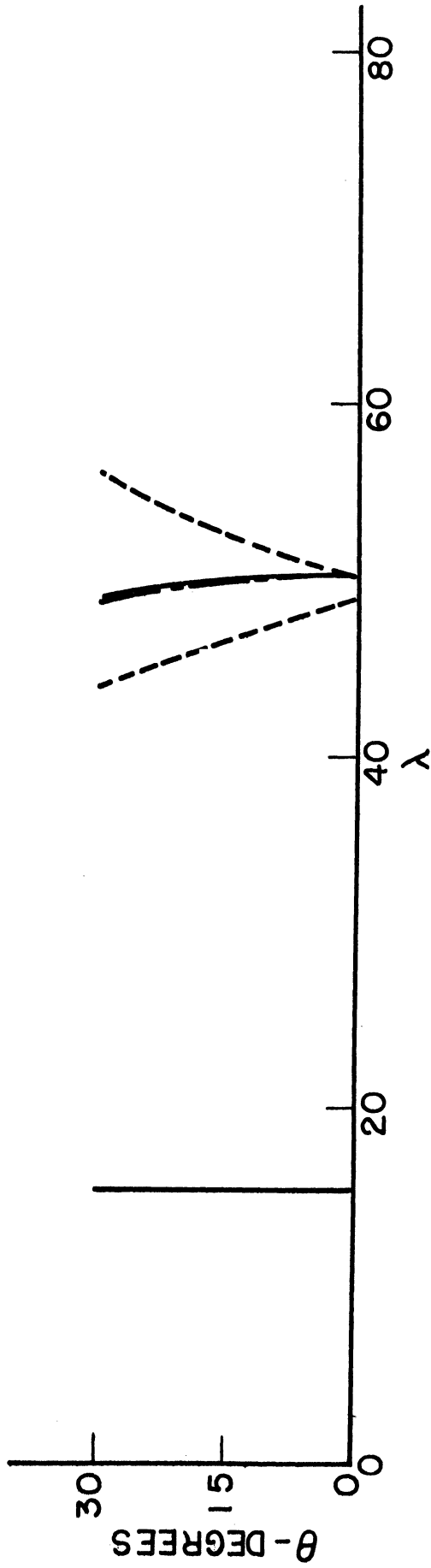
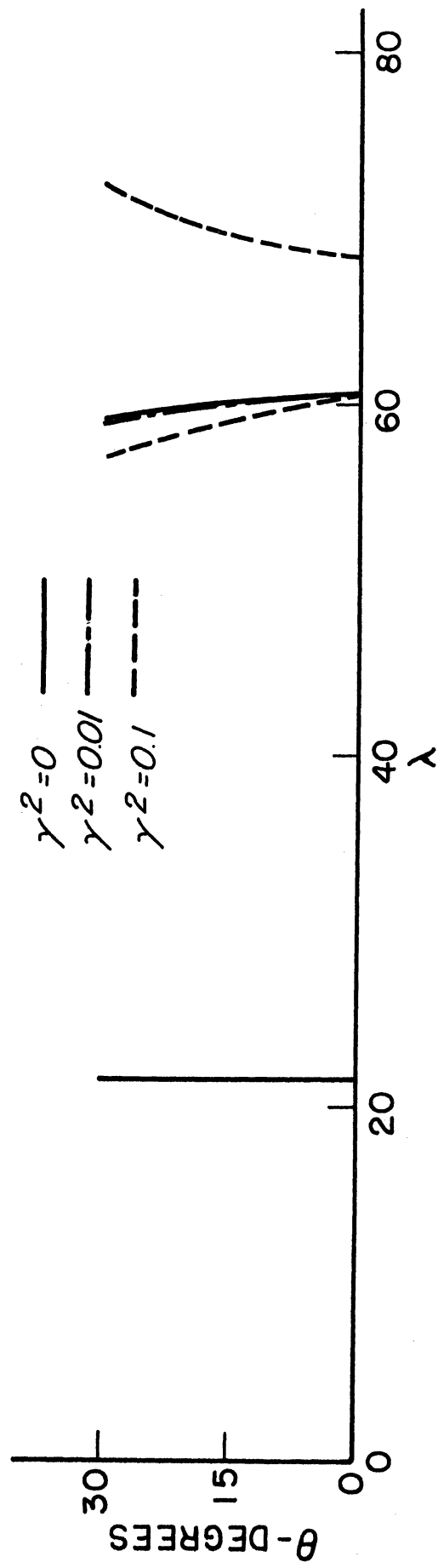


Fig. 4. Natural frequencies of nonrotating cantilever blade.  $\bar{e} = 0$ .



(a) Uniform Blade,  $\bar{\rho}_T=1, \bar{E}I_T=1$



(b) Tapered Blade,  $\bar{\rho}_T=0, \bar{E}I_T=0$

Fig. 5. Natural frequencies of nonrotating articulated blade.  $\bar{e} = 0$ .

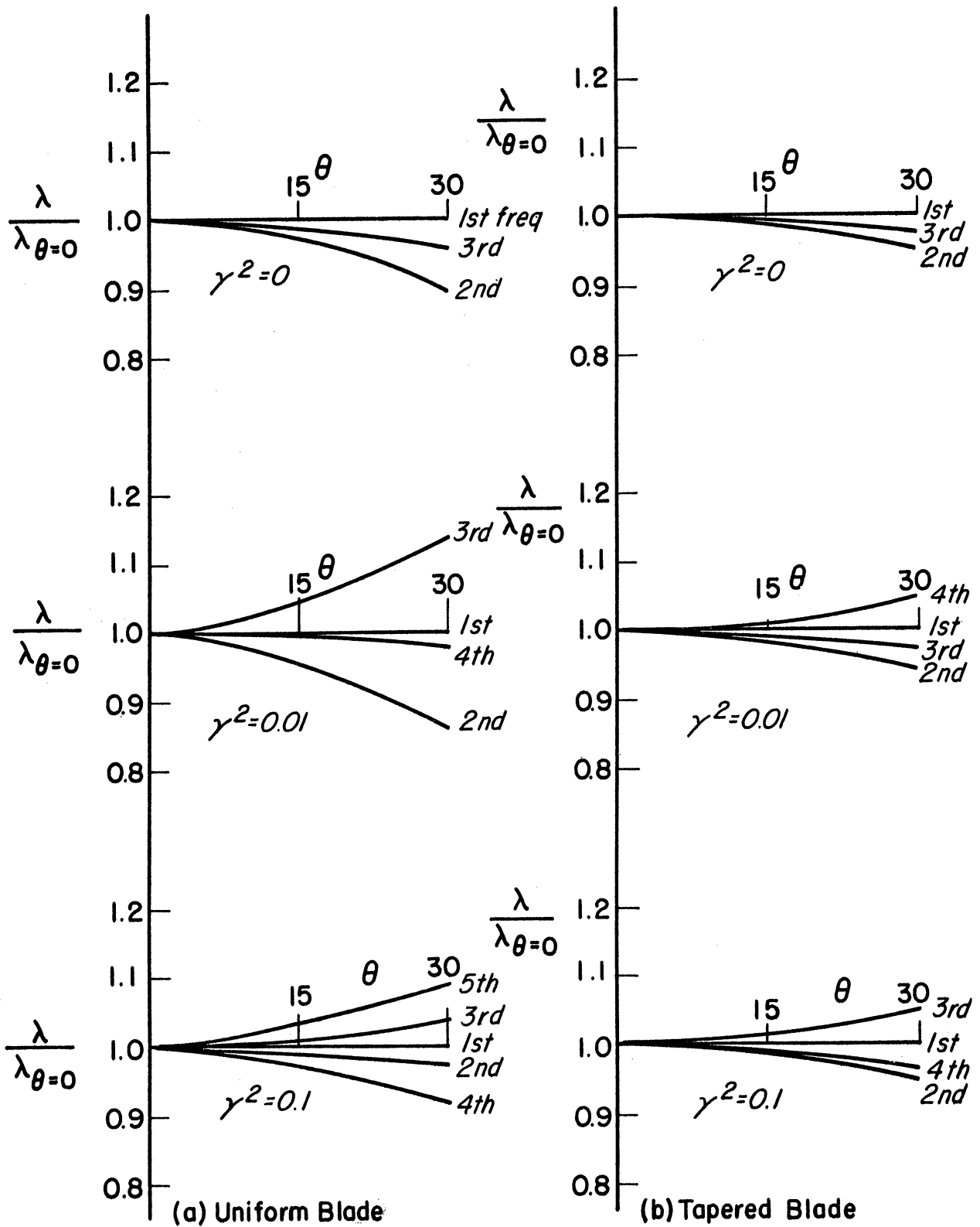


Fig. 6. Effect of twist on natural frequencies of nonrotating cantilever blade.  
 $\bar{e} = 0$ .

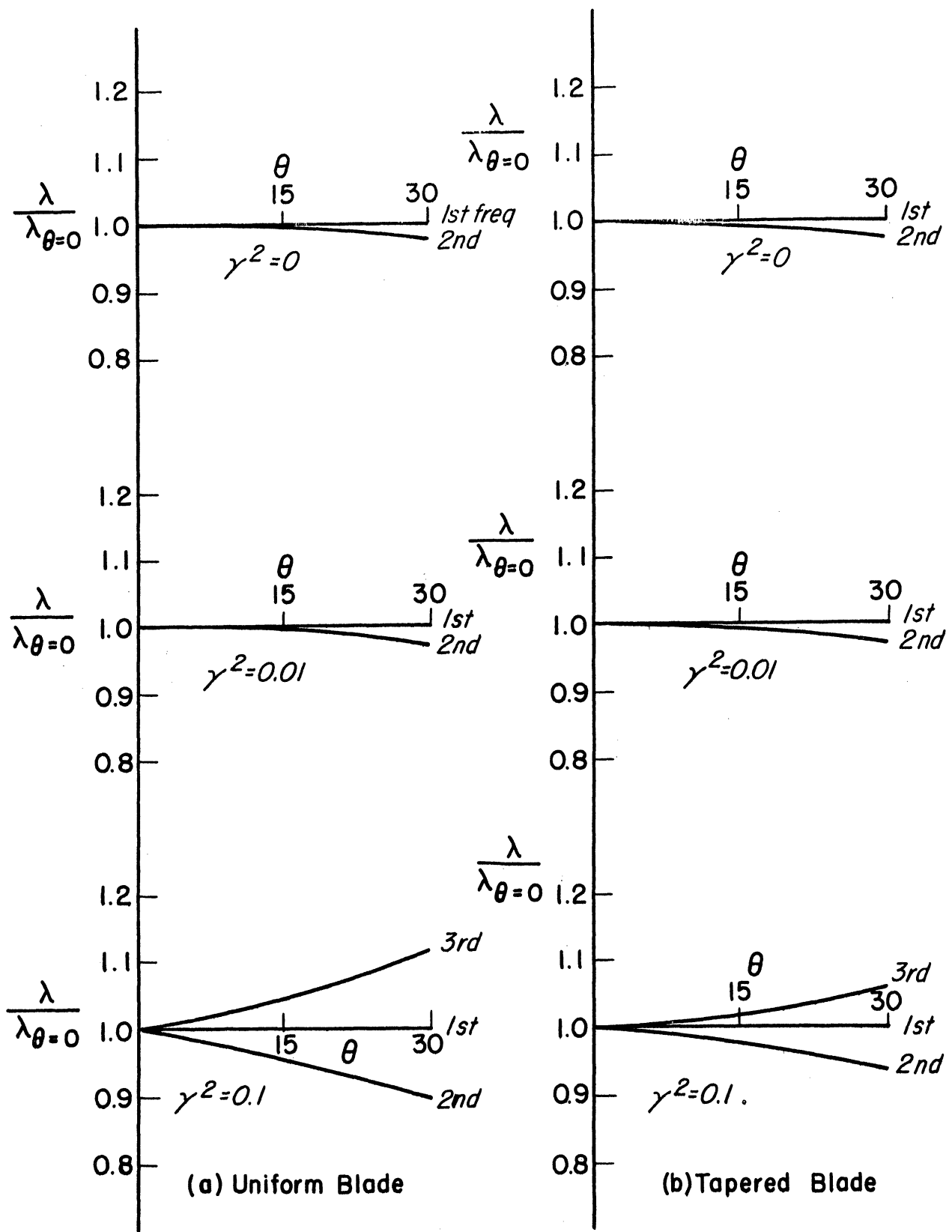


Fig. 7. Effect of twist on natural frequencies of nonrotating articulated blade.  $\bar{\epsilon} = 0$ .

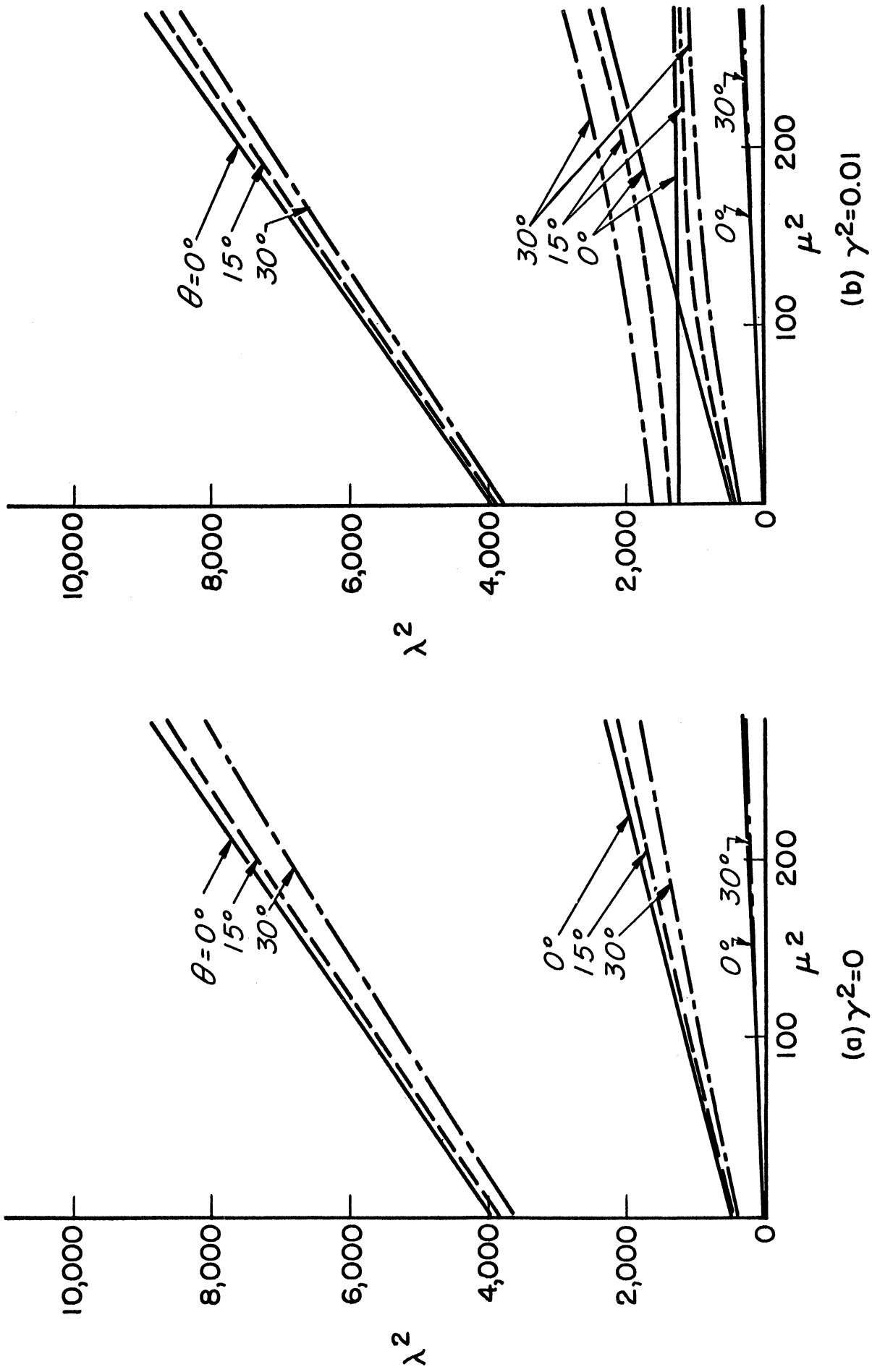
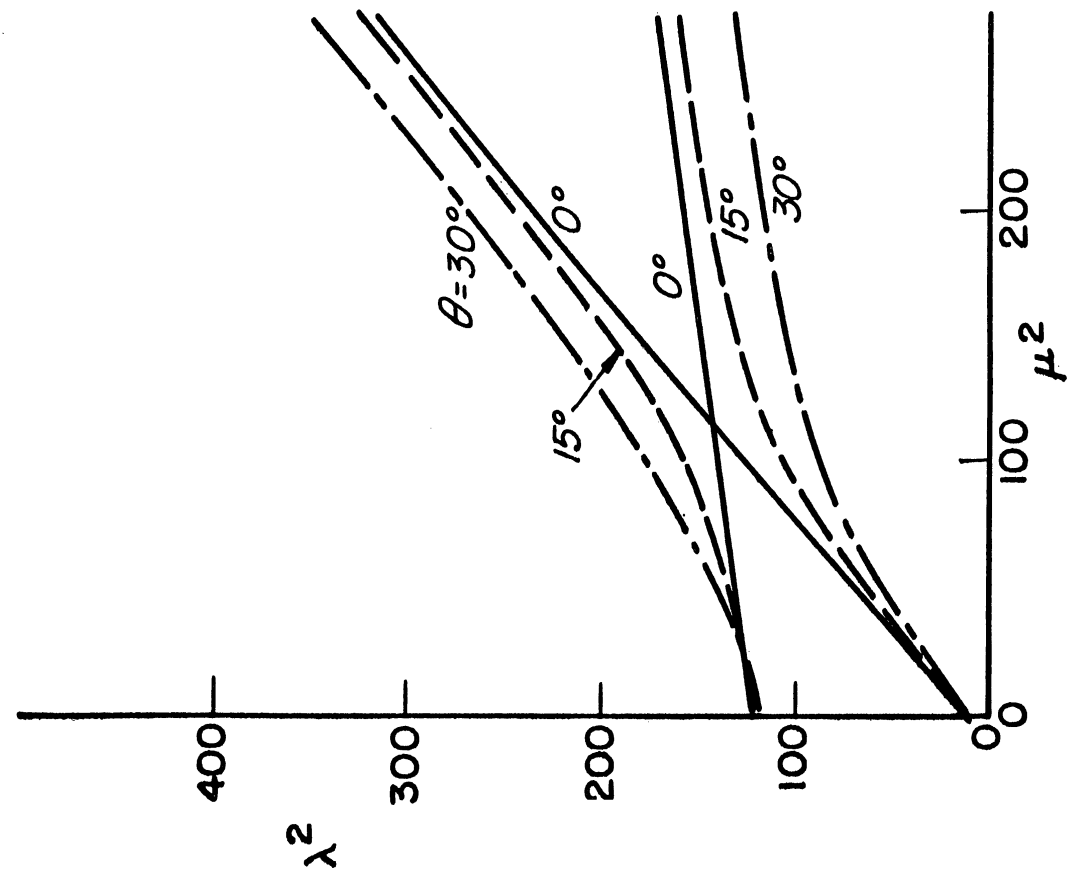
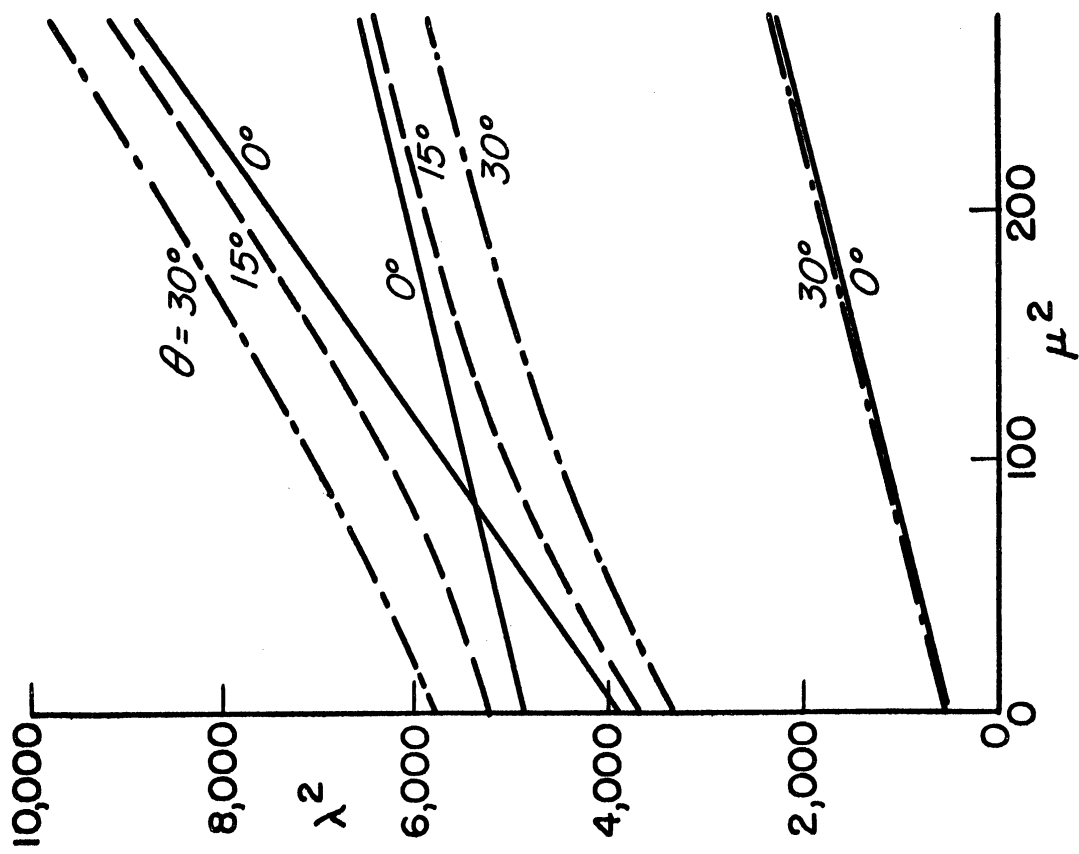


Fig. 8. Natural frequencies of rotating uniform cantilever blade.  $\bar{e} = 0$ ,  $\beta_{\text{T}} = 0$ .

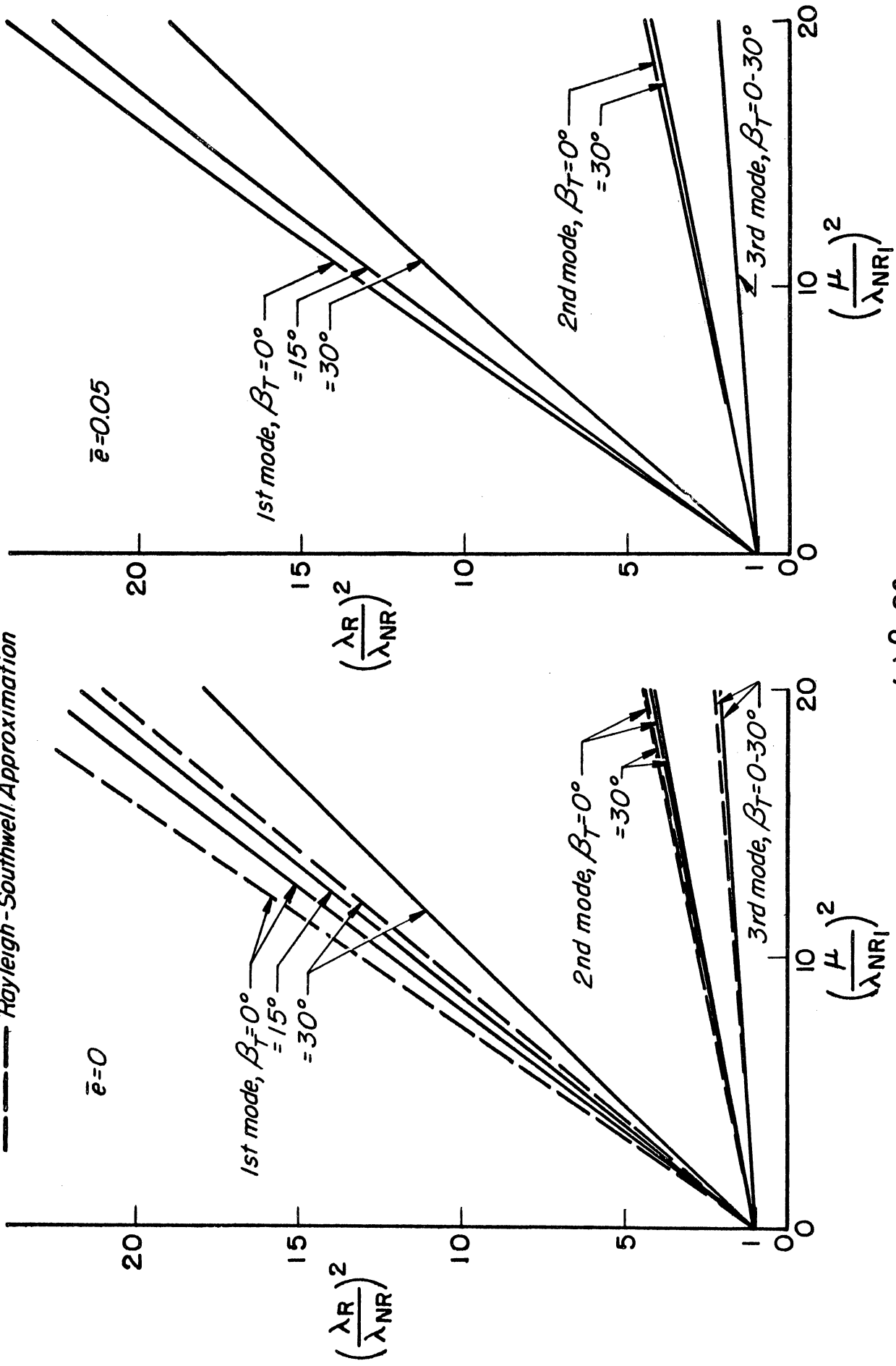


(c)  $\gamma^2 = 0.1$

Fig. 8. (Concluded)

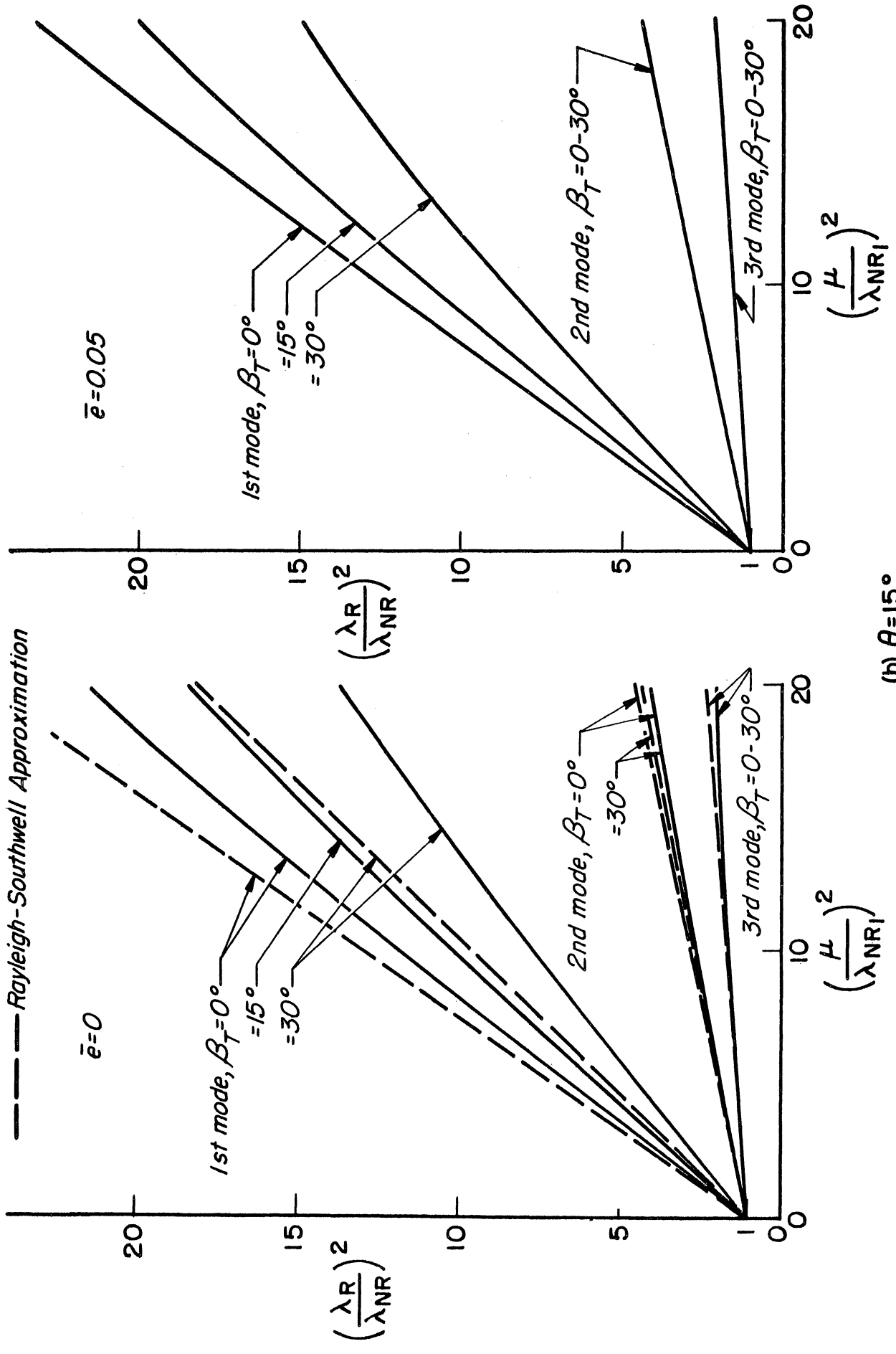


Rayleigh-Southwell Approximation



(a)  $\theta = 0^\circ$

Fig. 9. Frequency ratios for rotating uniform cantilever blade.  $\gamma^2 = 0$ .



(b)  $\theta = 15^\circ$

Fig. 9. (Continued)

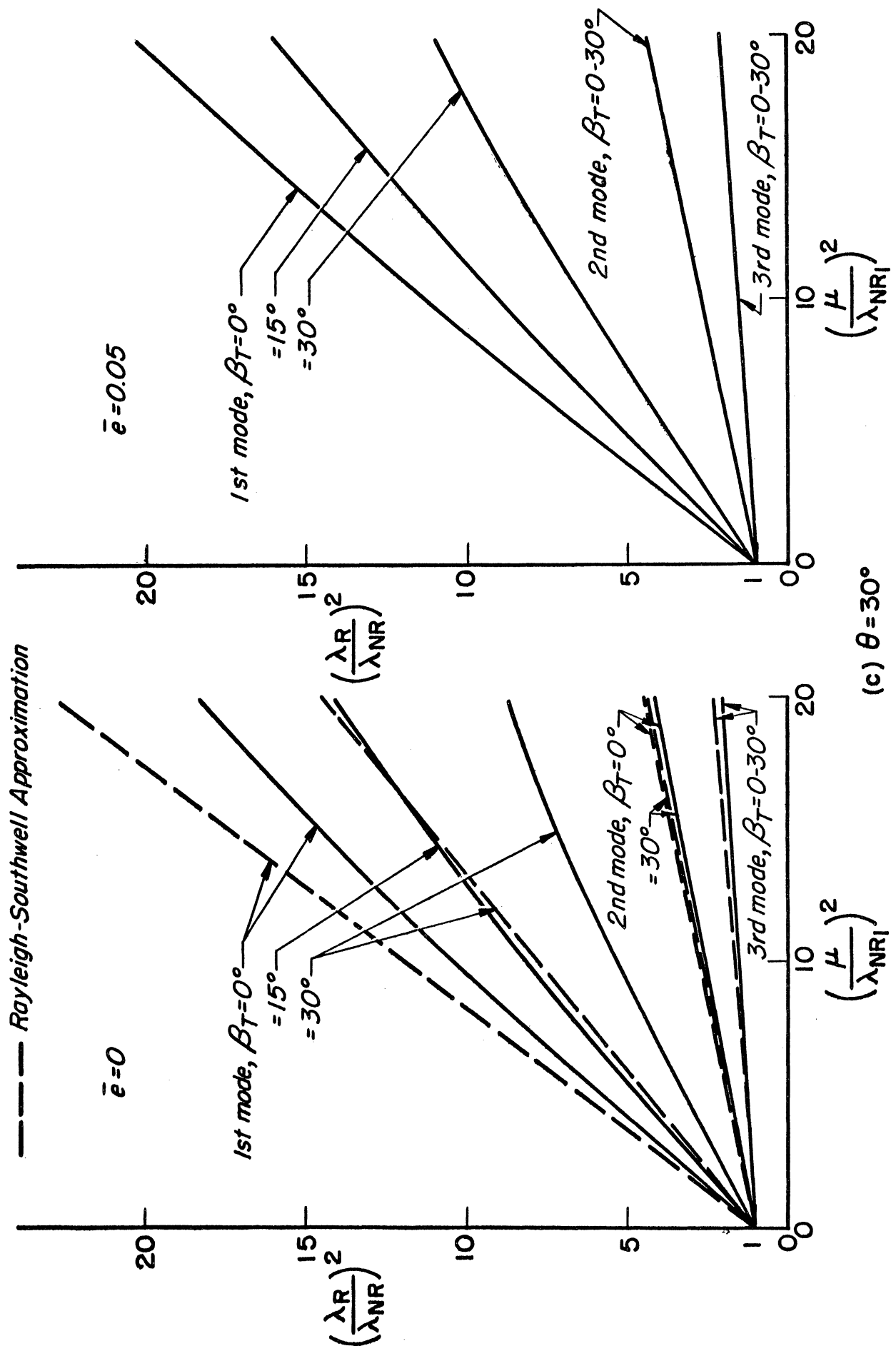


Fig. 9. (Concluded)

--- Rayleigh-Southwell Approximation

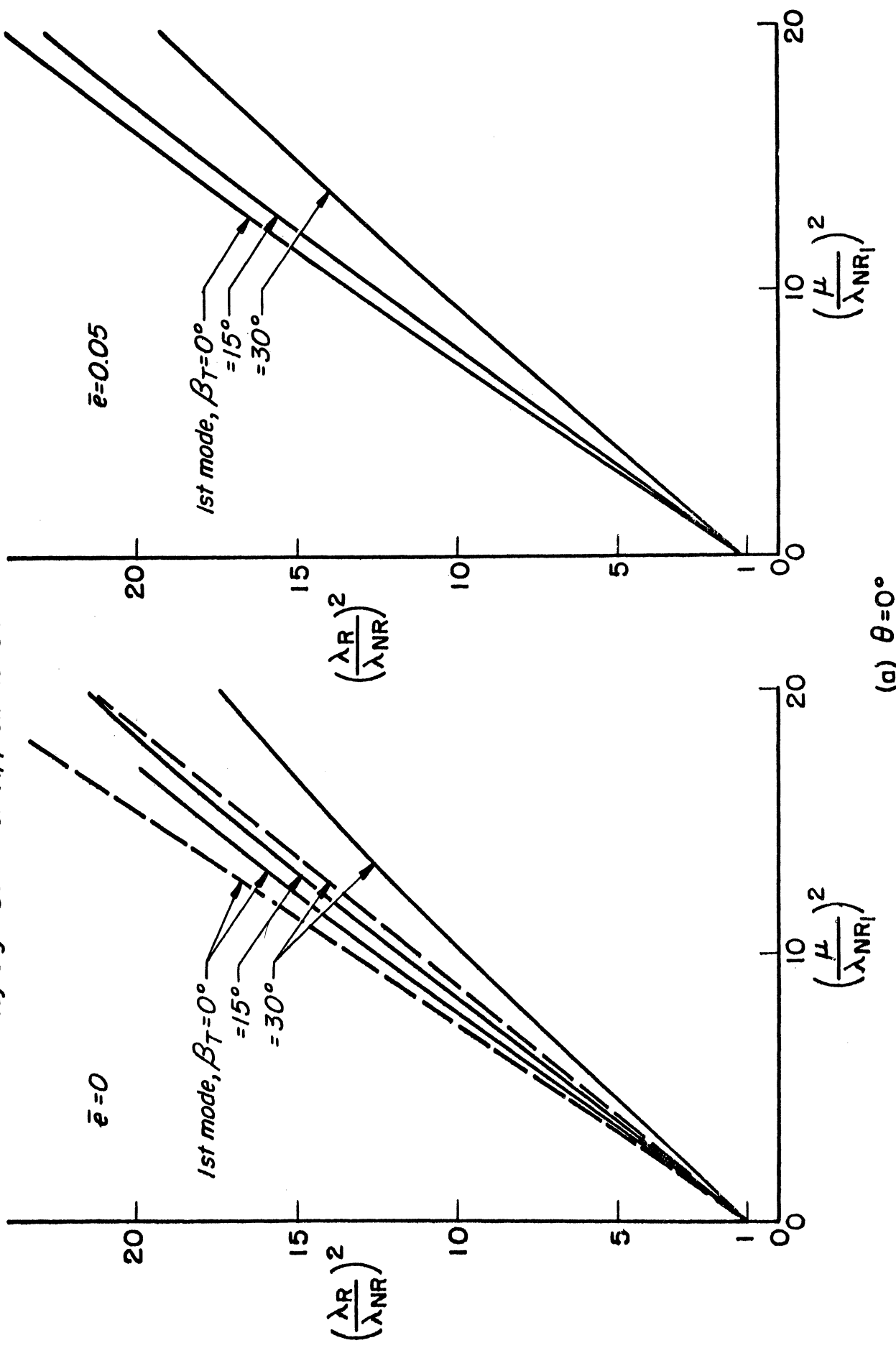


Fig. 10. Frequency ratios for rotating uniform cantilever blade.  $\gamma^2 = 0.01$ .

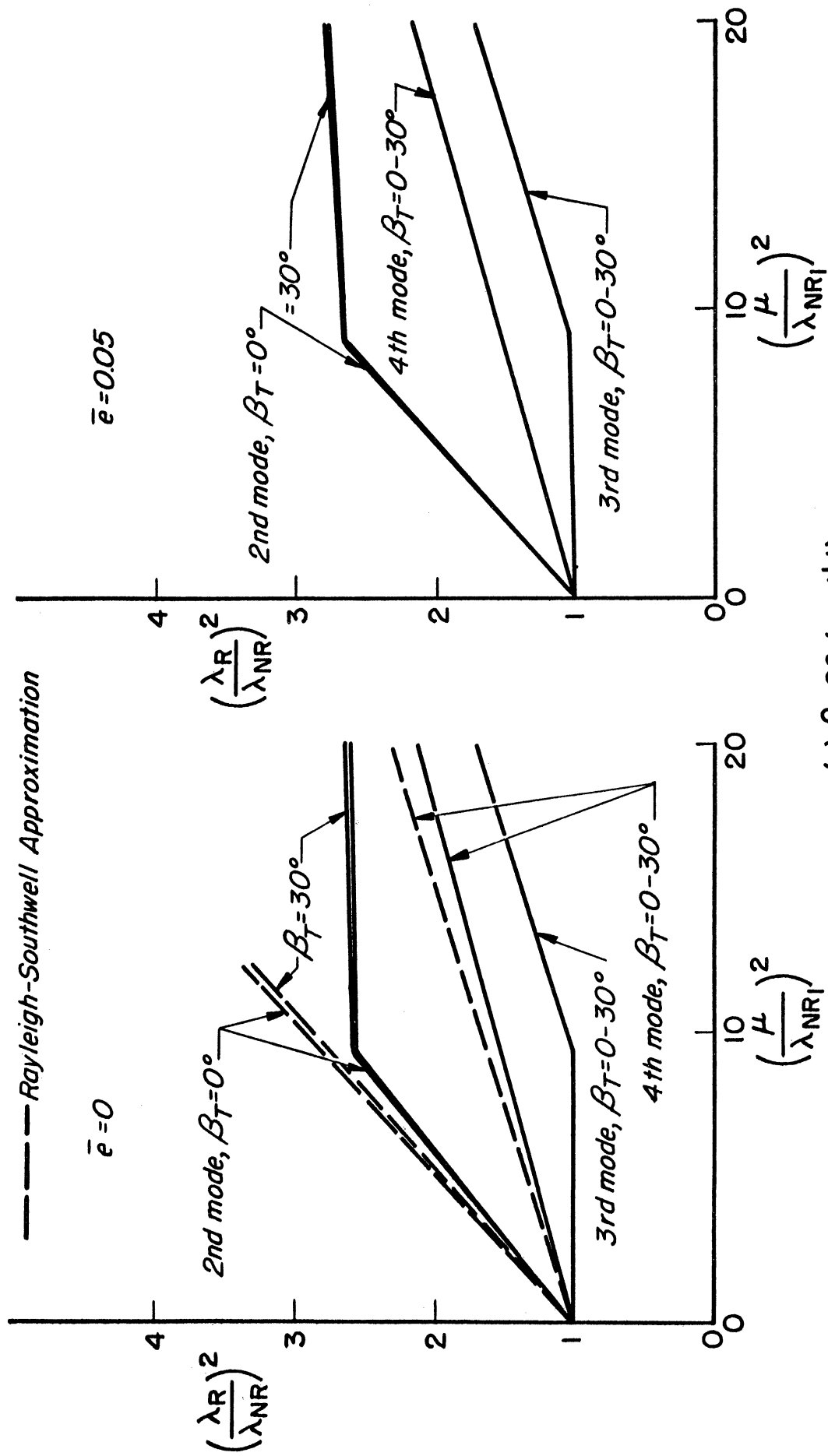


Fig. 10. (Continued)

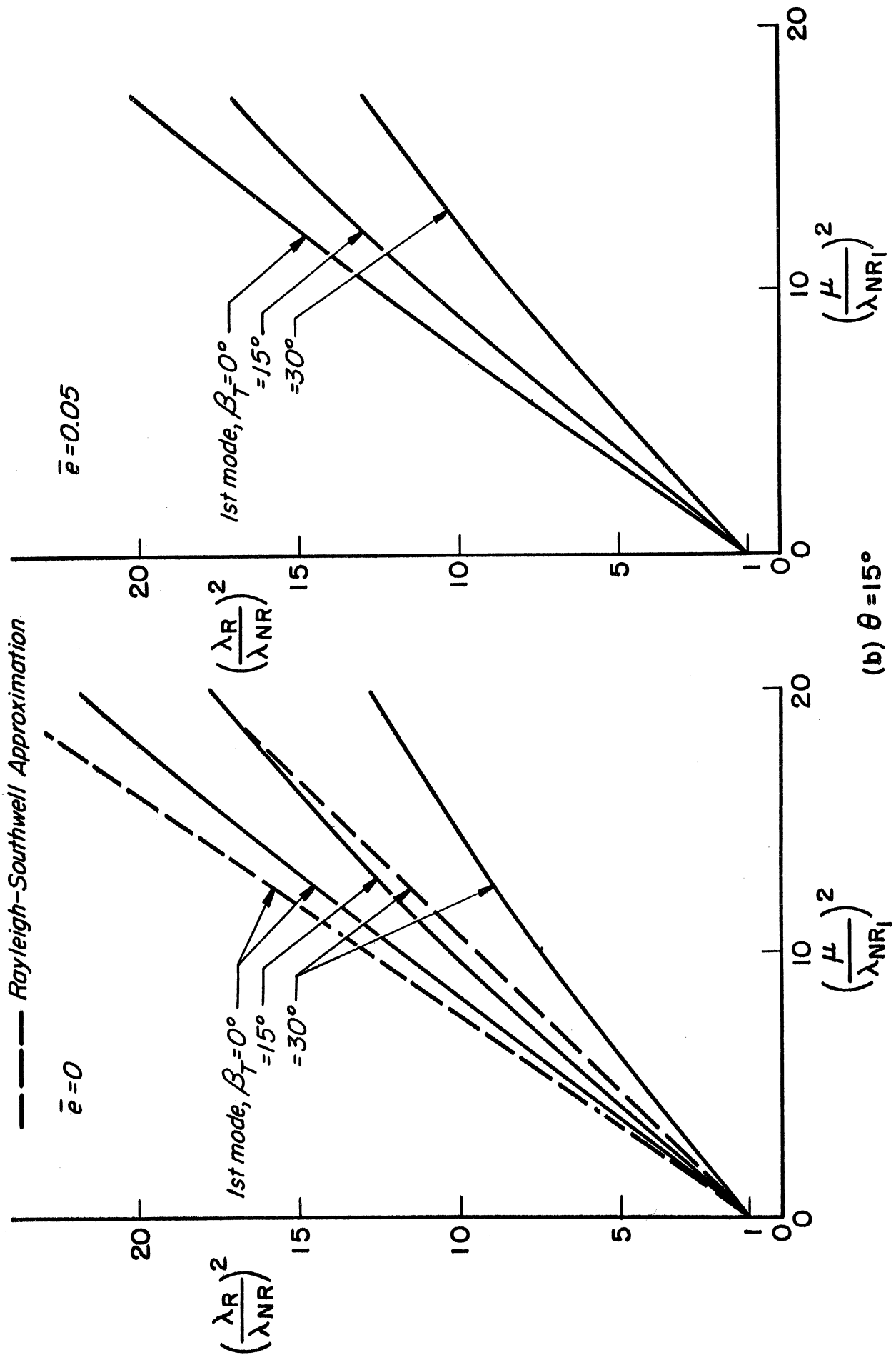
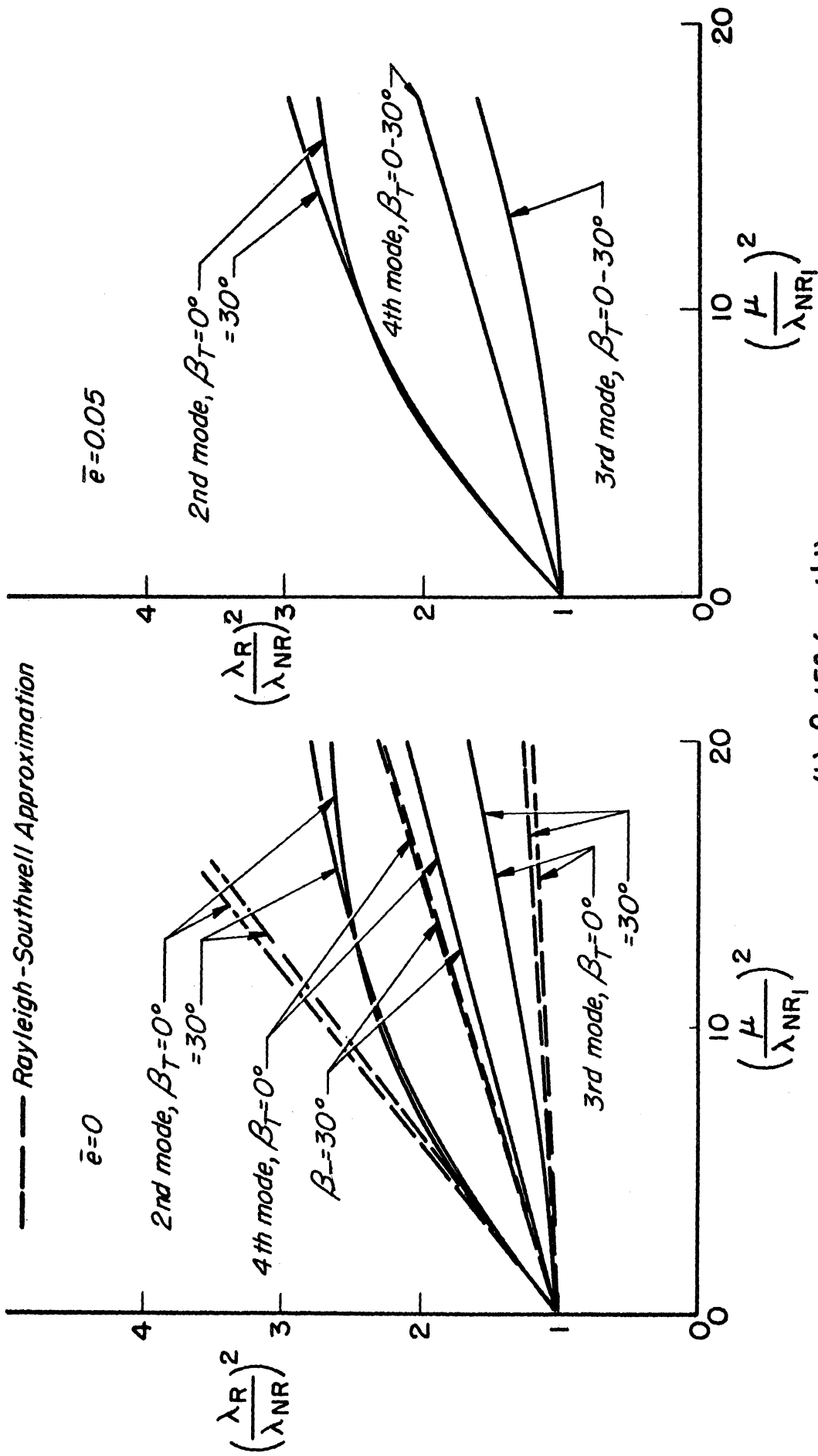


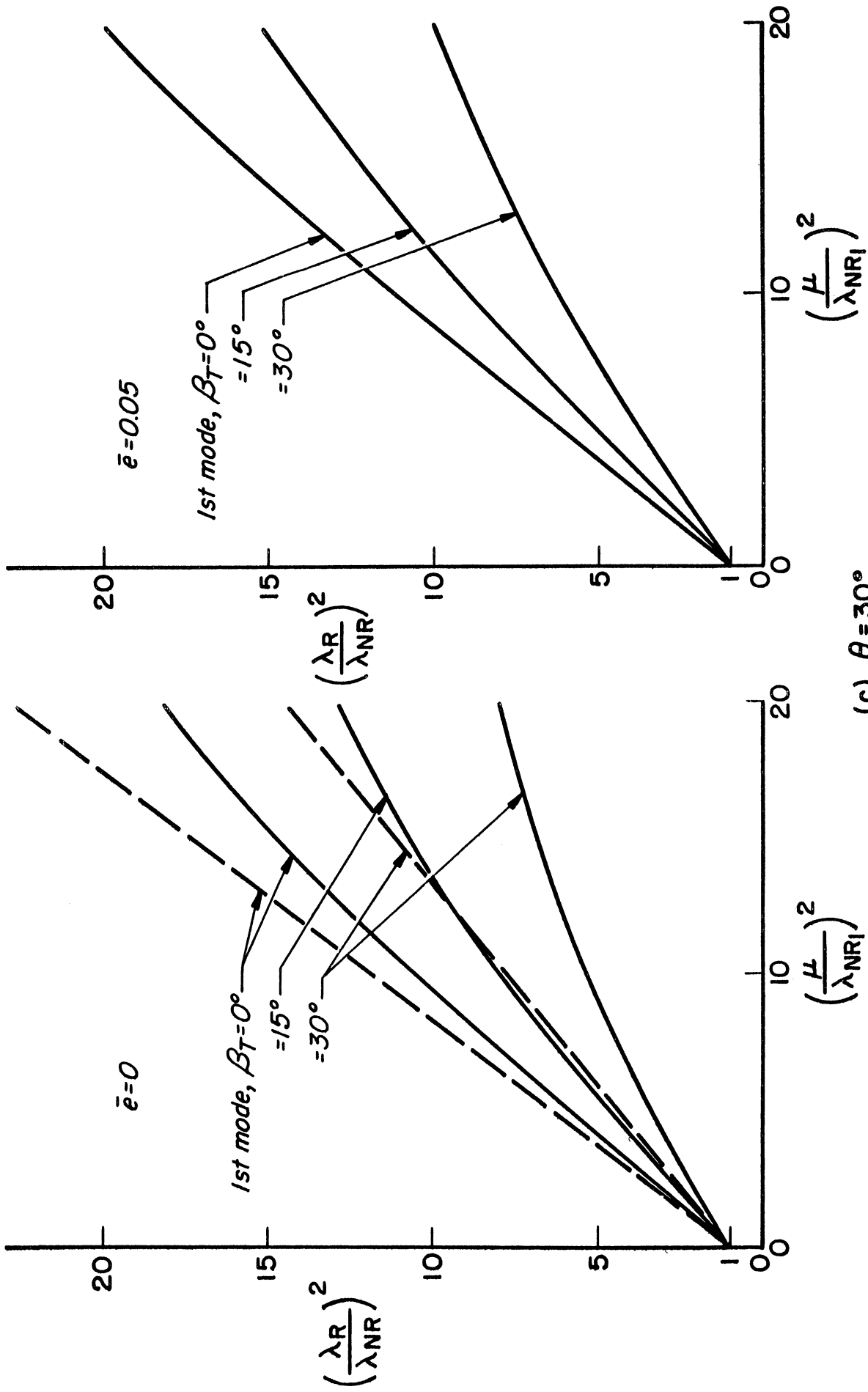
Fig. 10. (Continued)



(b)  $\theta = 15^\circ$  (cont'd)

Fig. 10. (Continued)

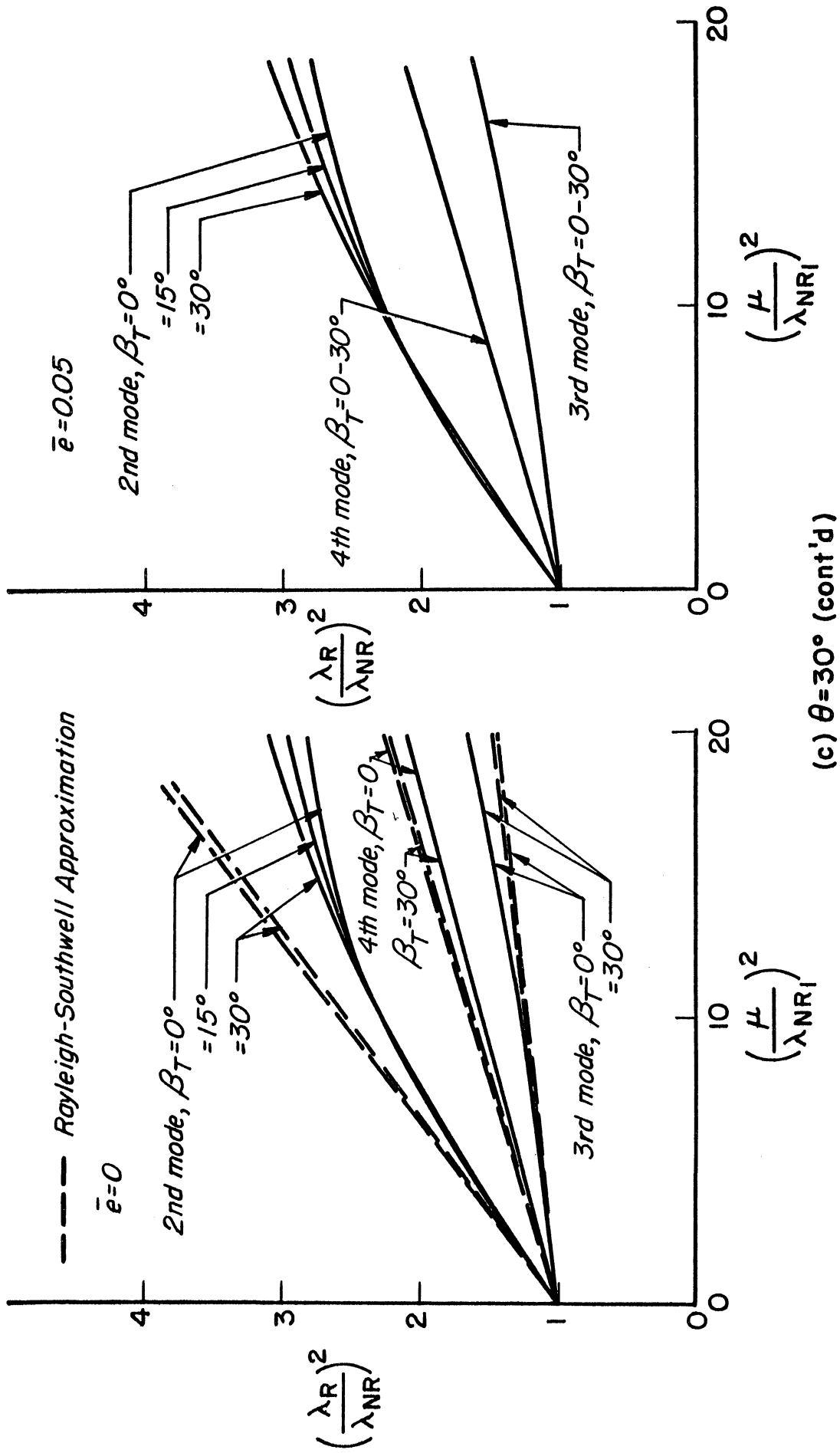
--- Rayleigh-Southwell Approximation



(c)  $\theta = 30^\circ$

Fig. 10. (Continued)





(c)  $\theta = 30^\circ$  (cont'd)

Fig. 10. (Concluded)

--- Rayleigh-Southwell Approximation

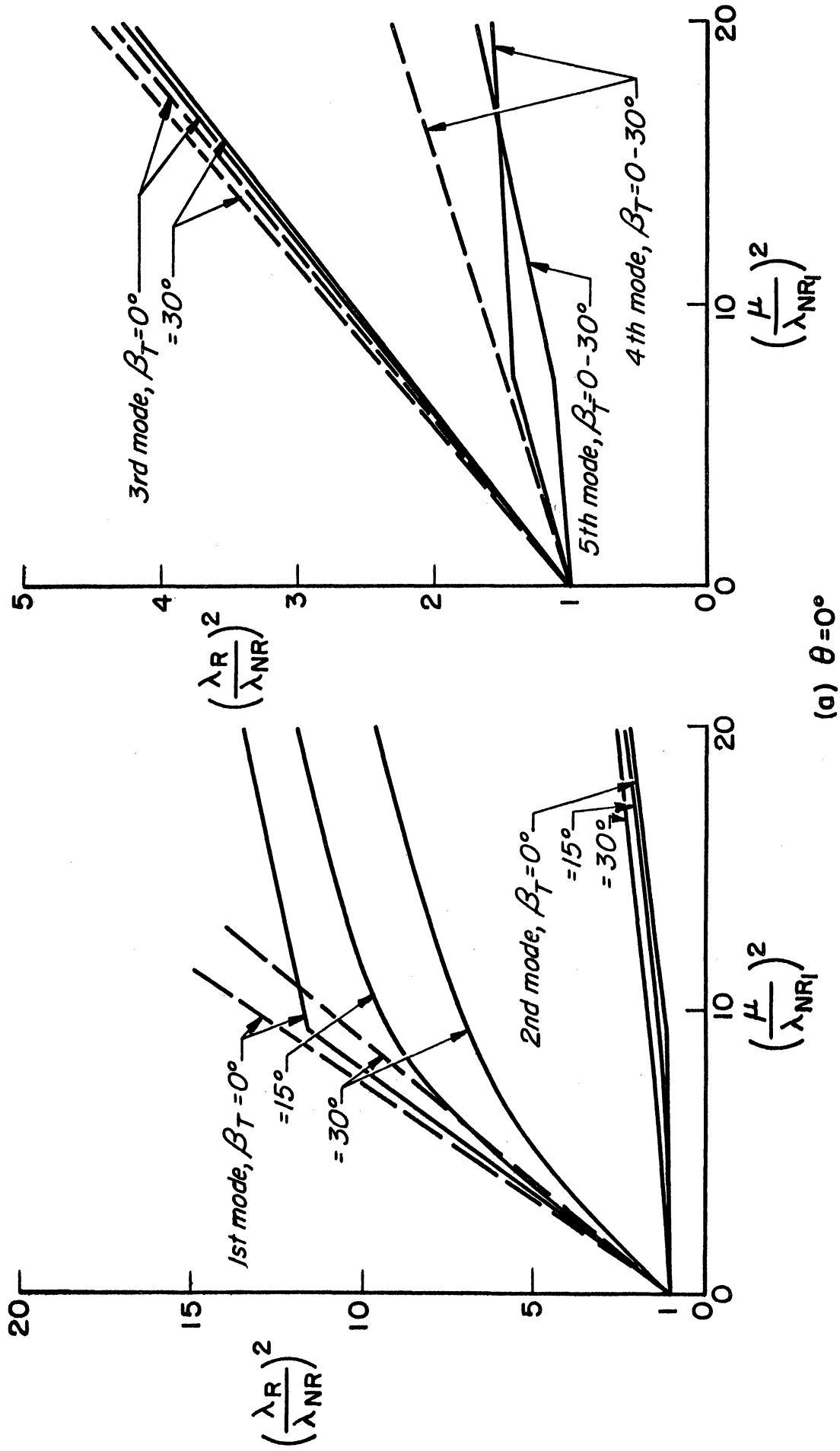


Fig. 11. Frequency ratios for rotating uniform cantilever blade.  $\gamma^2 = 0.1$ ,  $\bar{e} = 0$ .

--- Rayleigh-Southwell Approximation

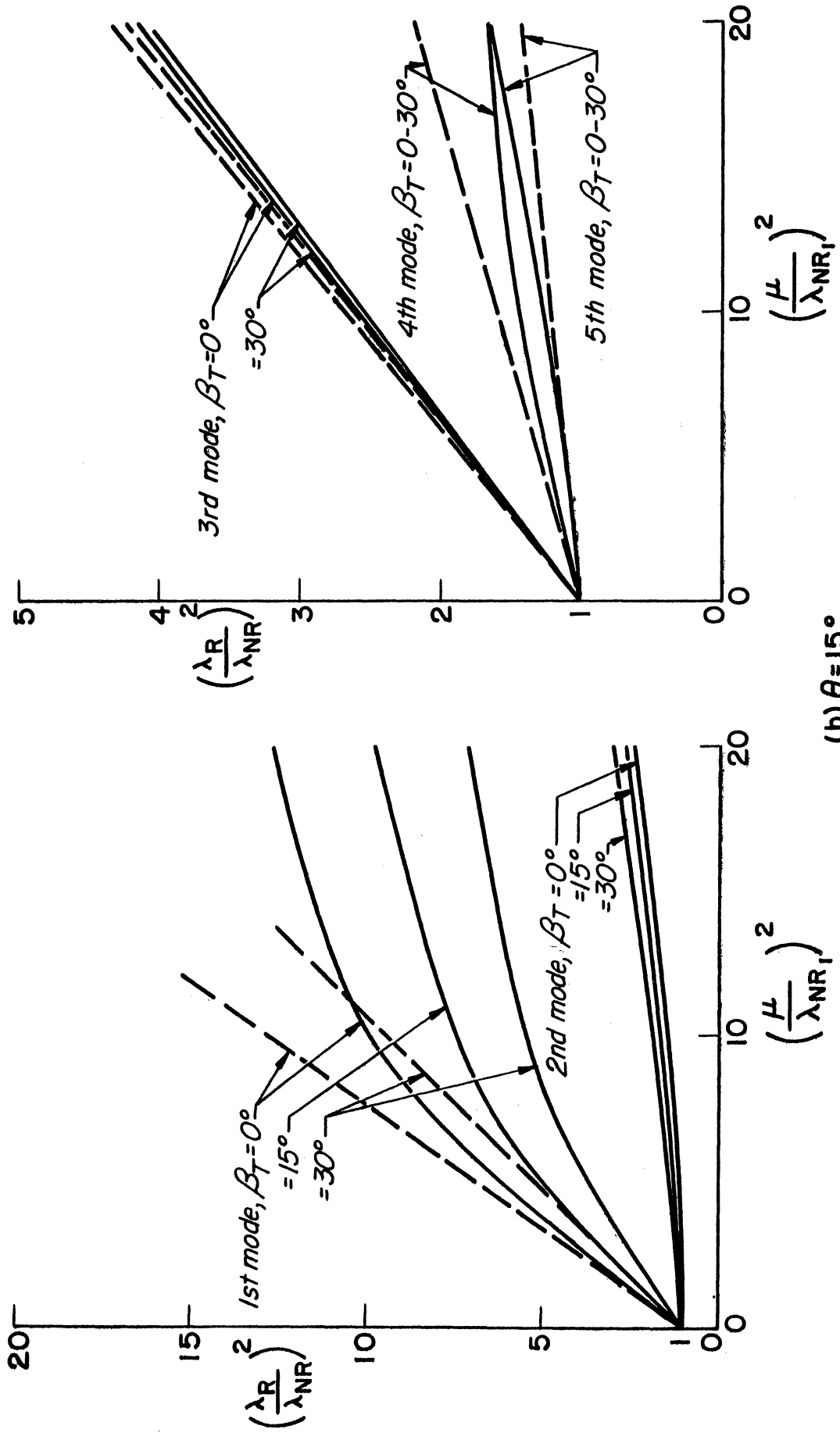
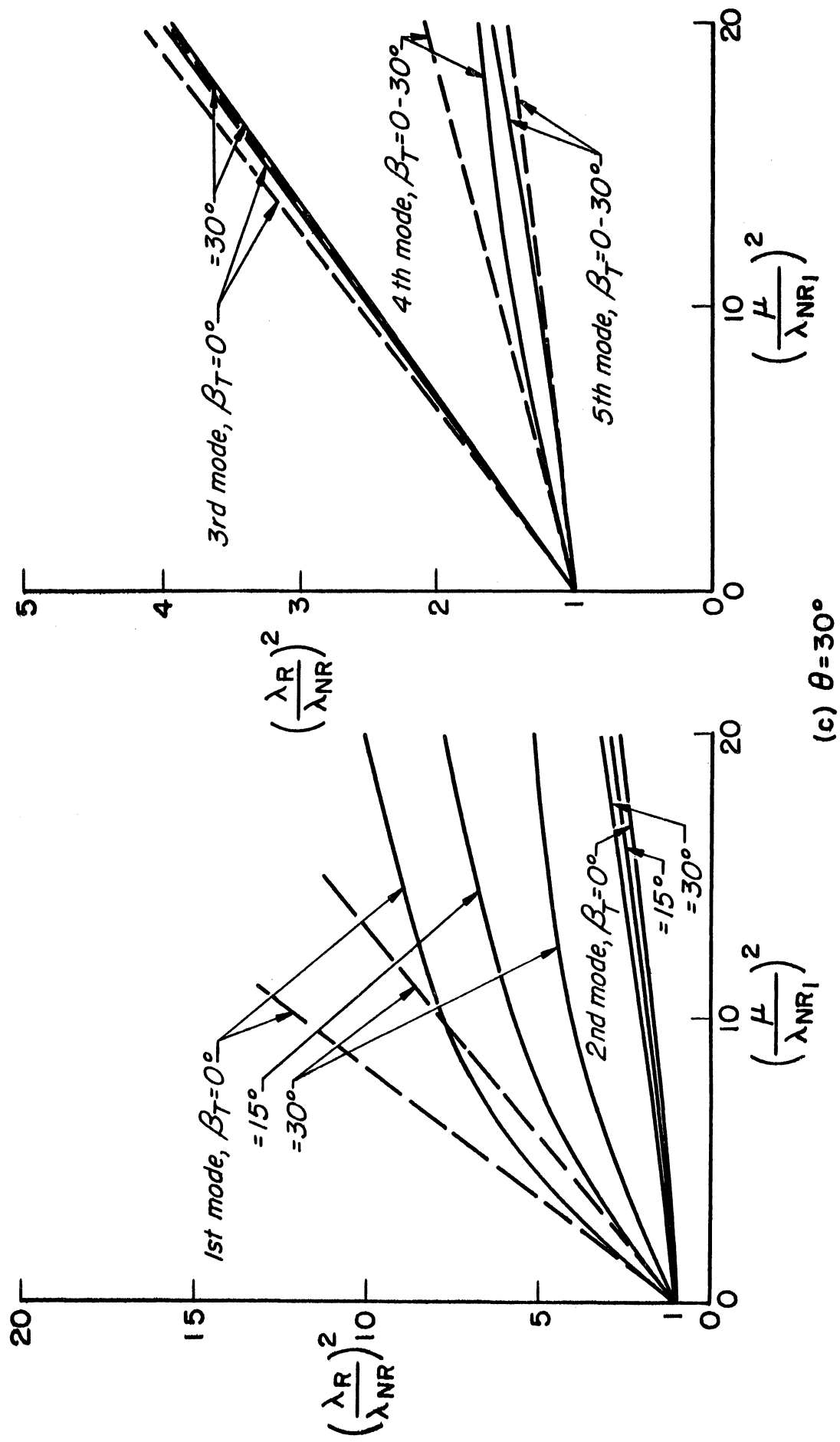


Fig. 11. (Continued)

— Rayleigh-Southwell Approximation



(c)  $\theta = 30^\circ$

Fig. 11. (Concluded)

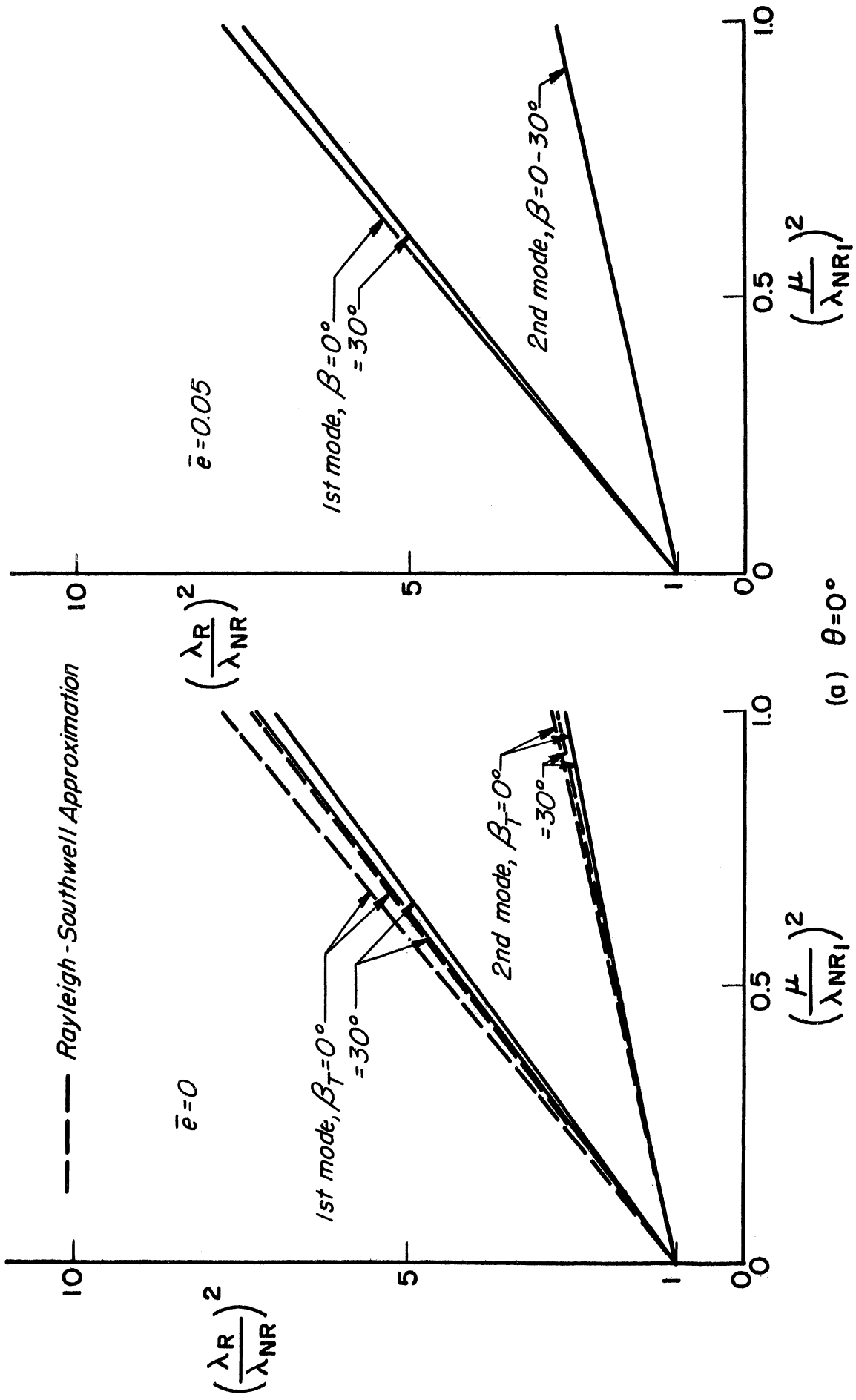
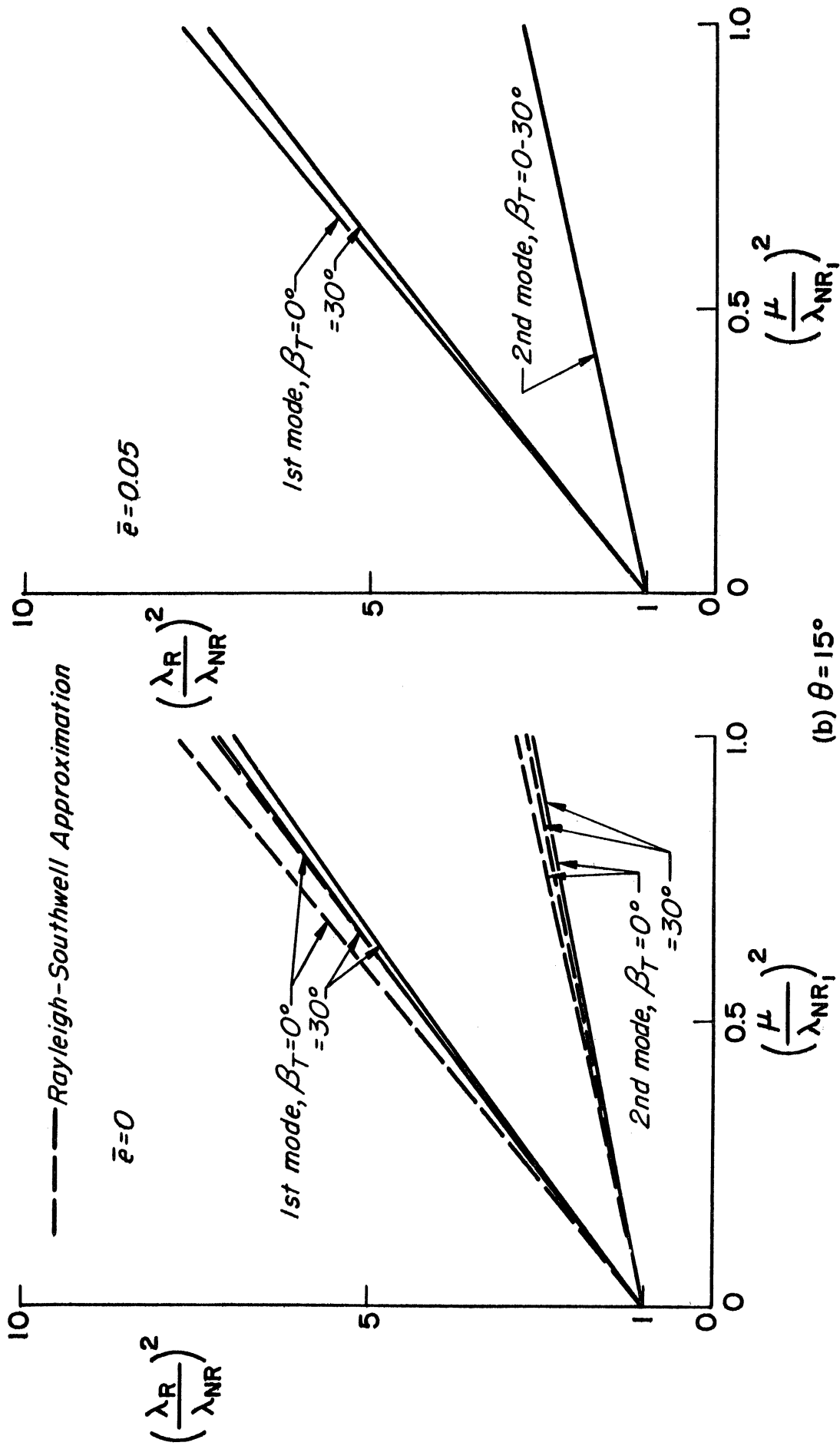


Fig. 12. Frequency ratios for rotating uniform articulated blade.  $\gamma^2 = 0$ .



(b)  $\theta = 15^\circ$

Fig. 12. (Continued)

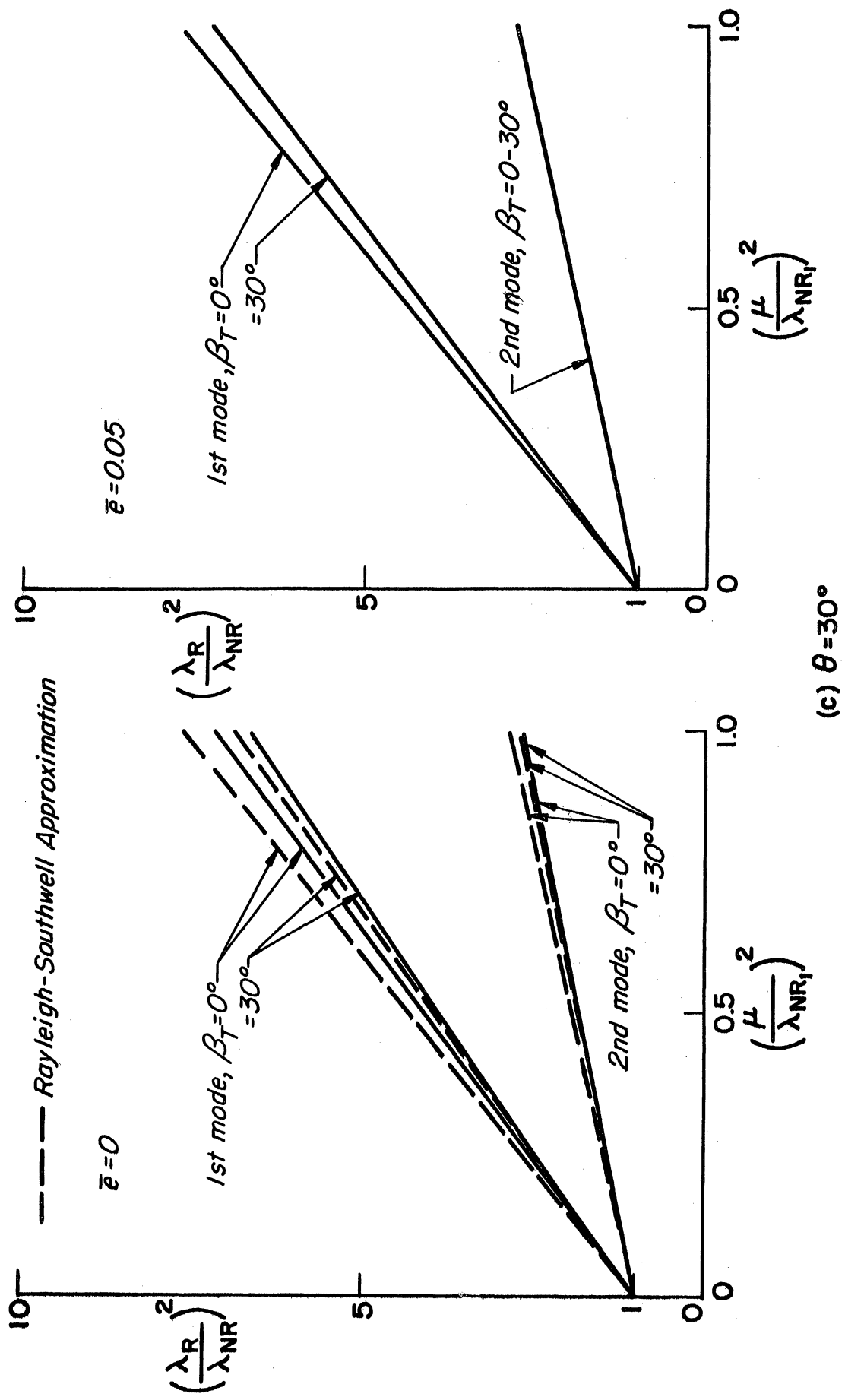


Fig. 12. (Concluded)

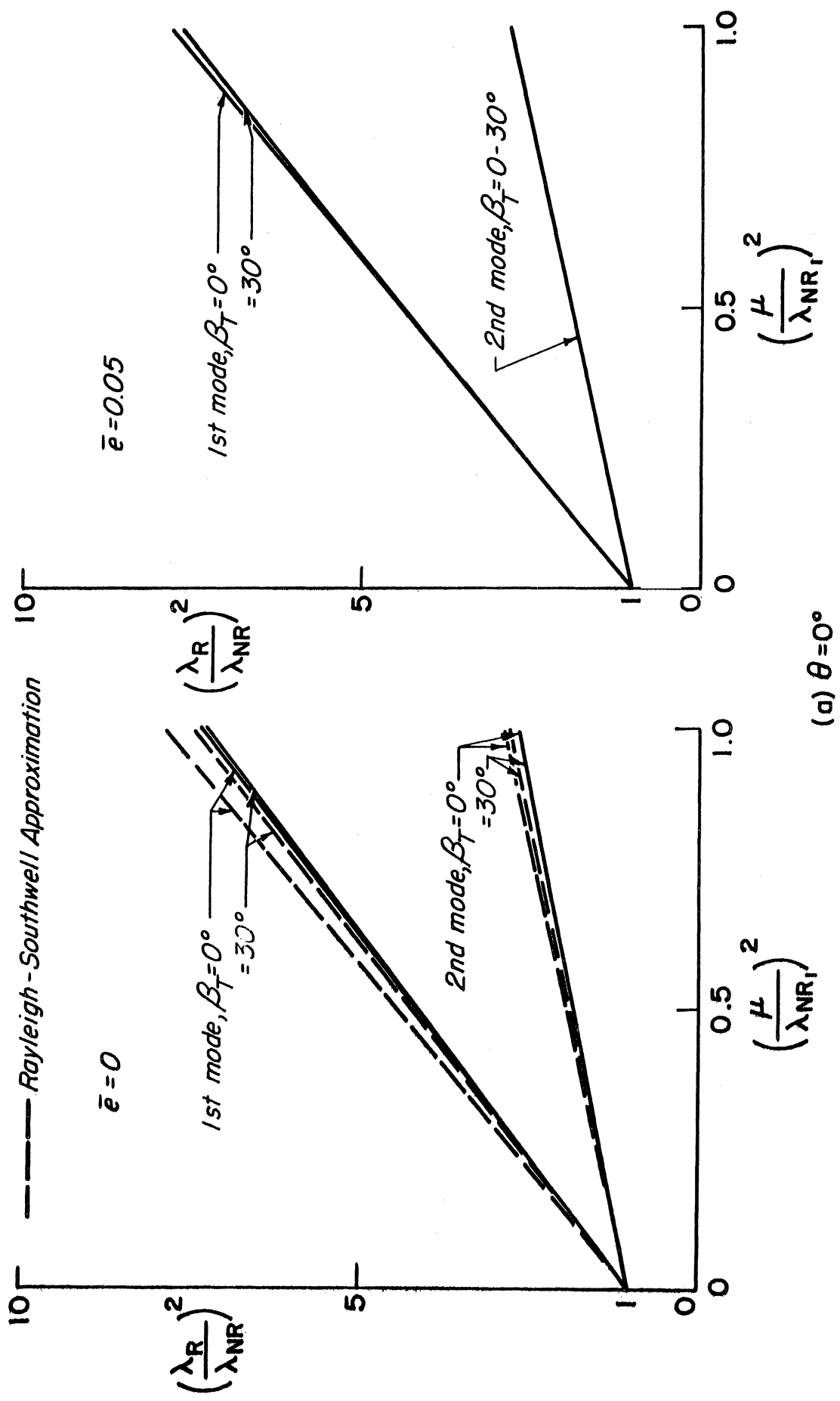
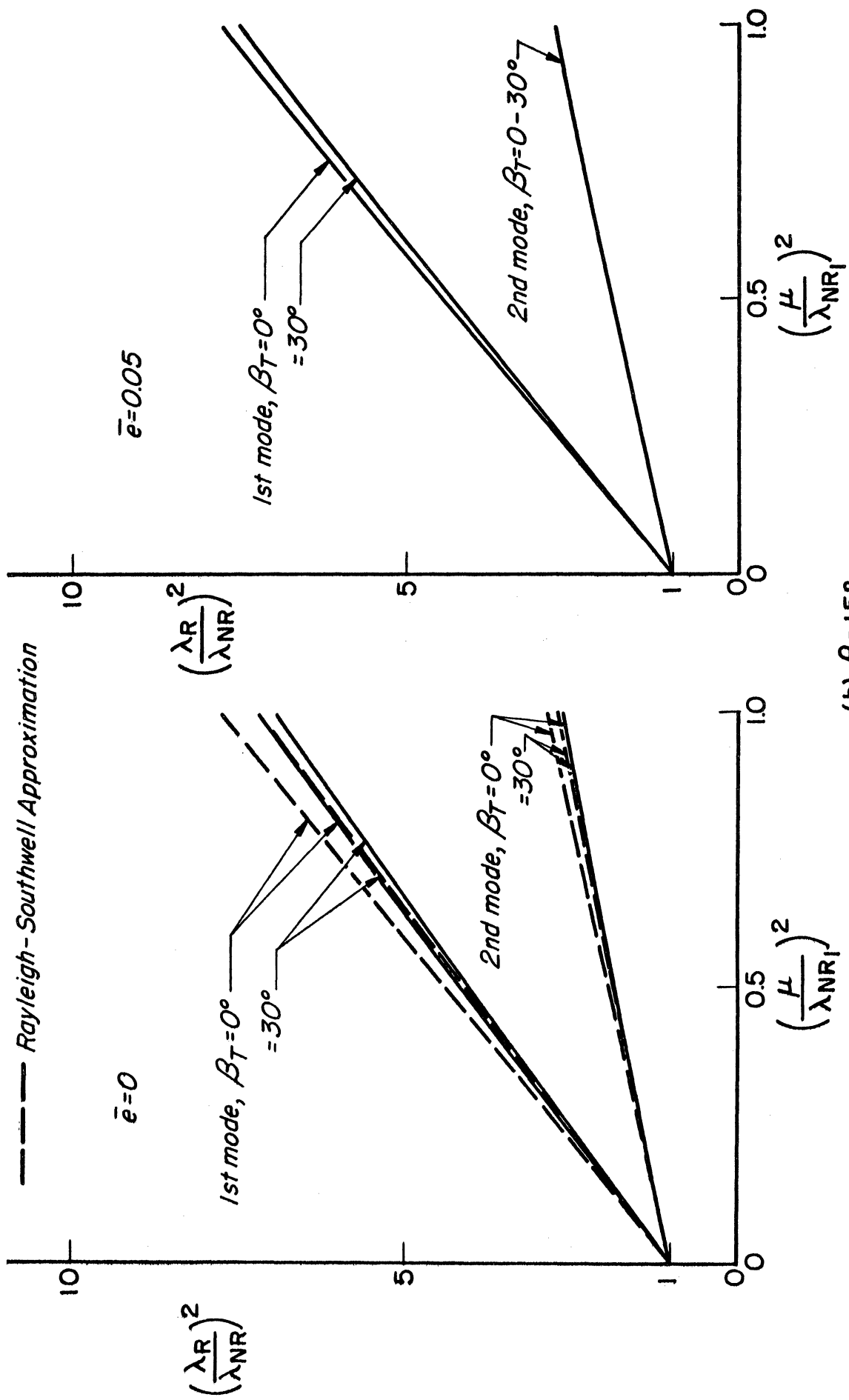


Fig. 13. Frequency ratios for rotating uniform articulated blade.  $\gamma^2 = 0.01$ .





(b)  $\theta = 15^\circ$

Fig. 13. (Continued)

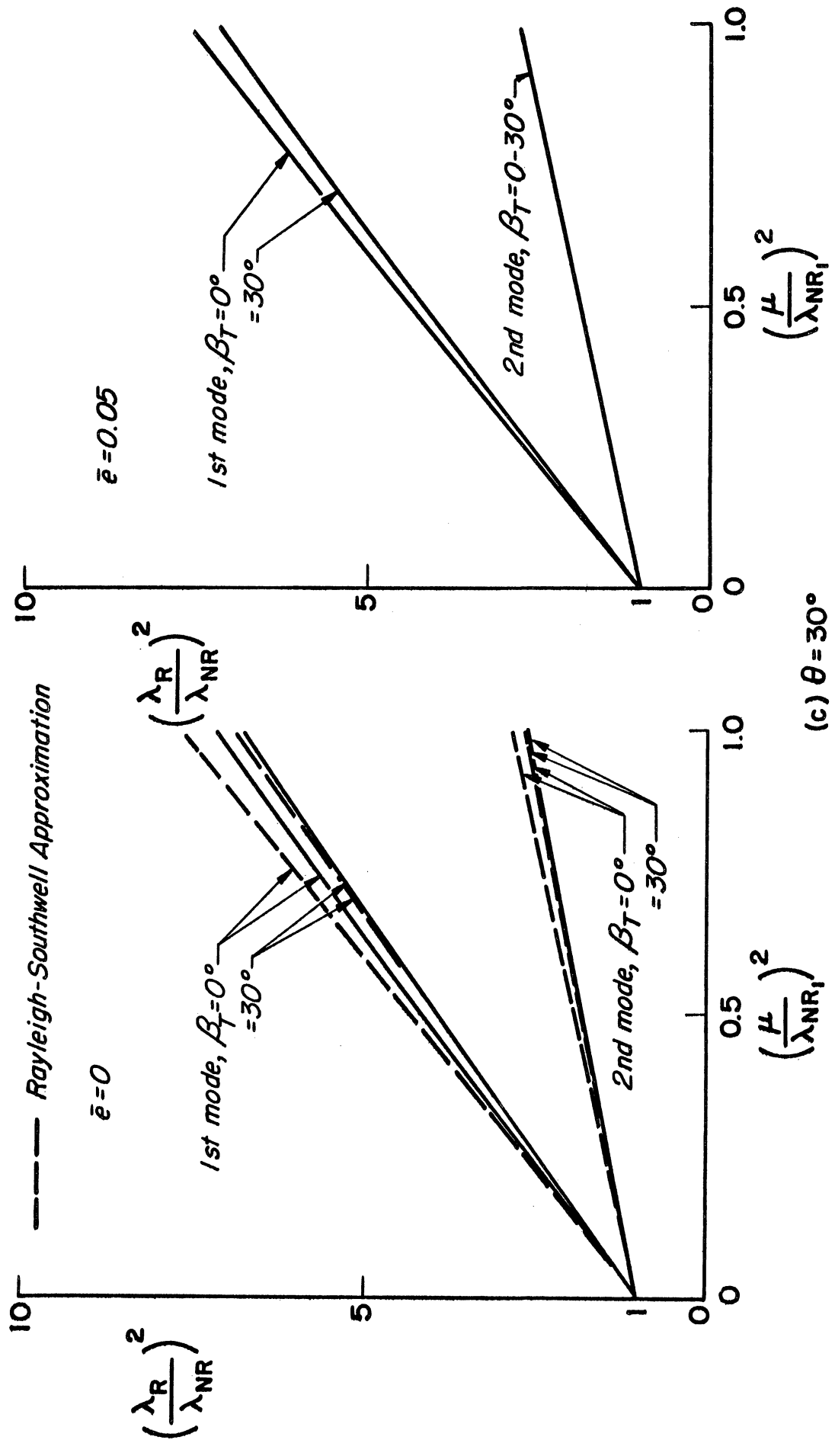


Fig. 13. (Concluded)

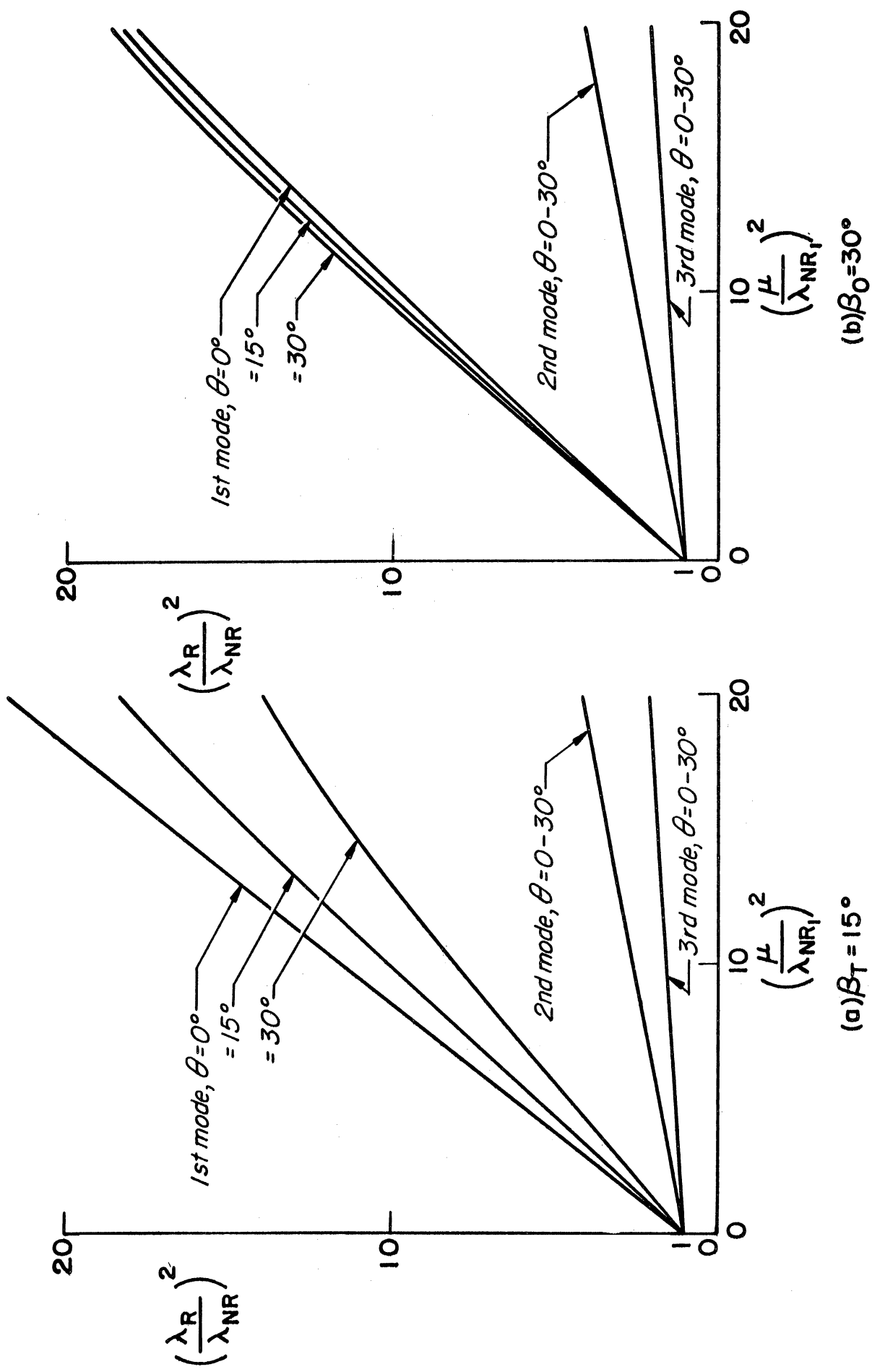


Fig. 14. Influence of twist on frequency ratios for rotating uniform cantilever blade.  $\gamma^2 = 0$ ,  $\bar{e} = 0$ .

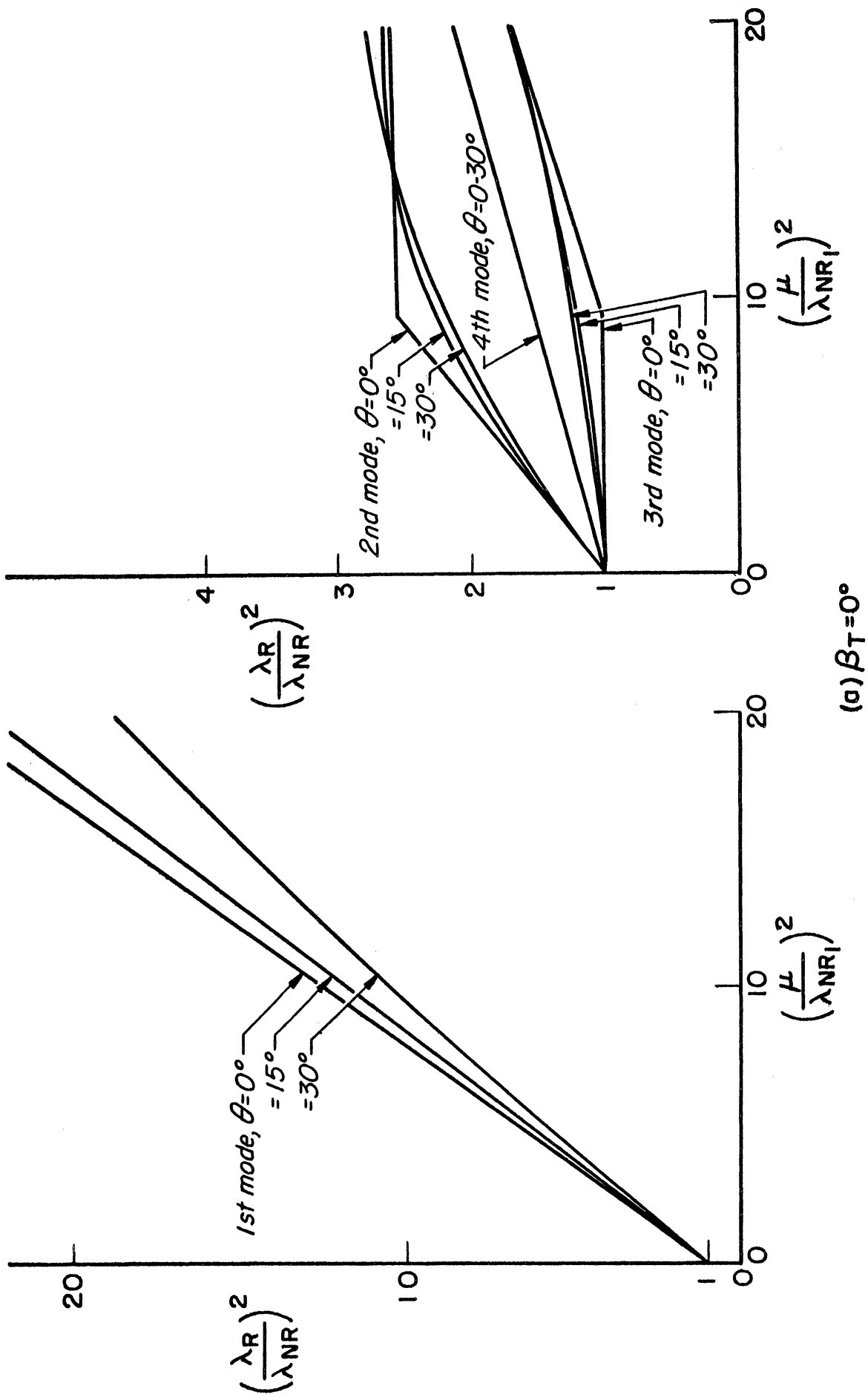
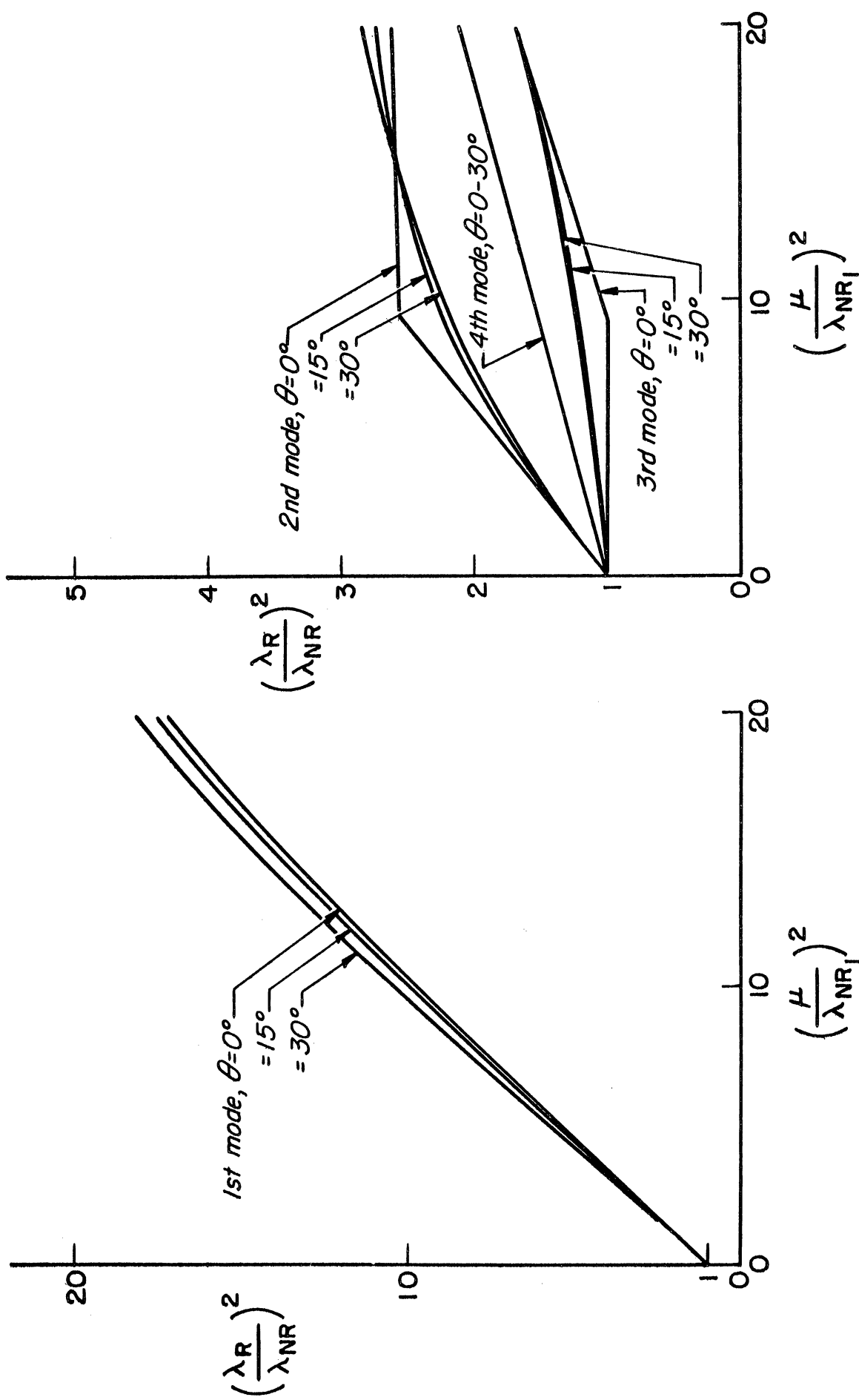


Fig. 15. Influence of twist on frequency ratios for rotating uniform cantilever blade.  $\gamma^2 = 0.01$ ,  $\bar{e} = 0$ .



(b)  $\beta_0 = 30^\circ$

Fig. 15. (Concluded)

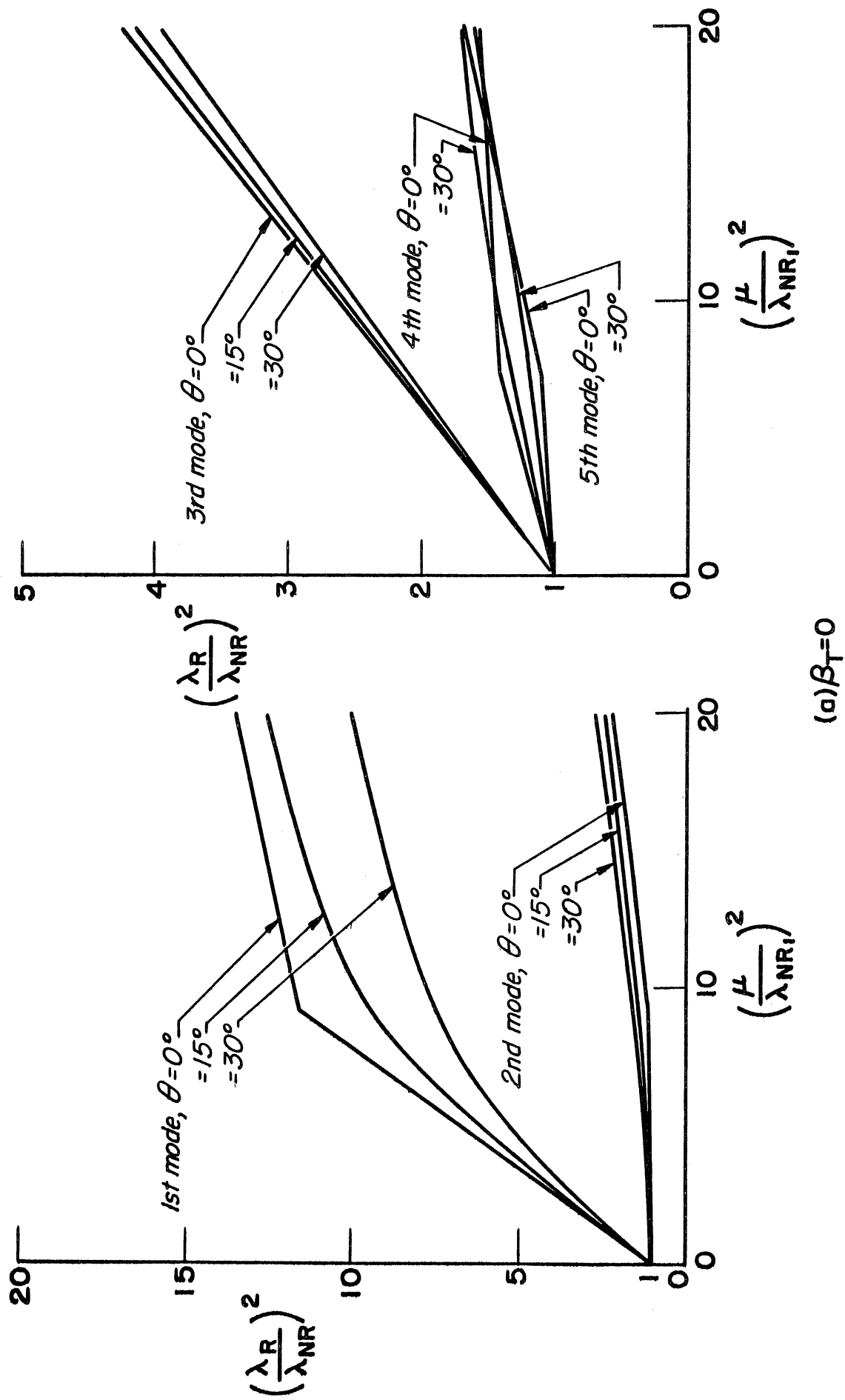


Fig. 16. Influence of twist on frequency ratios for rotating uniform cantilever blade.  $\gamma^2 = 0.1$ ,  $\bar{e} = 0$ .

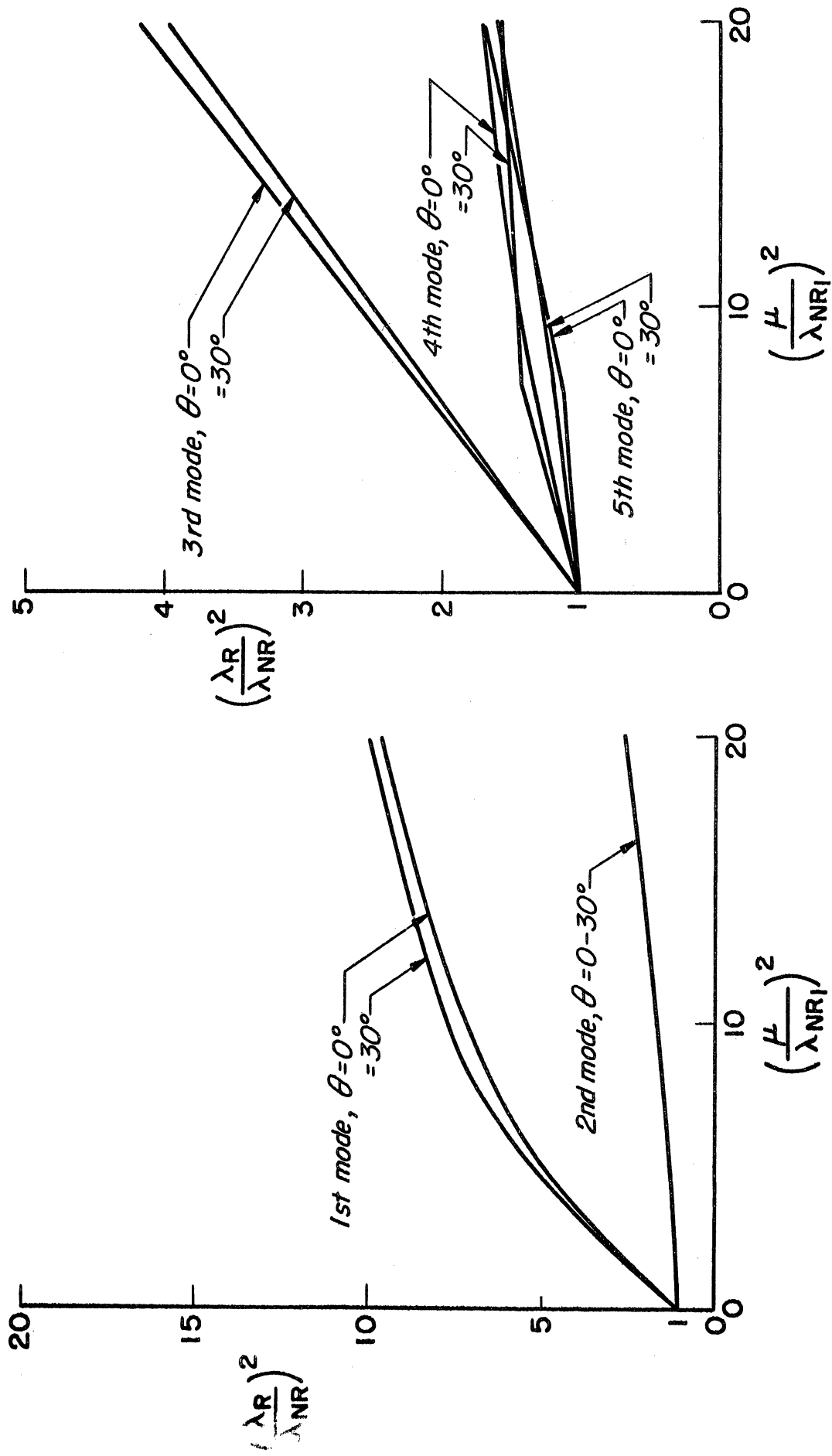


Fig. 16. (Concluded)

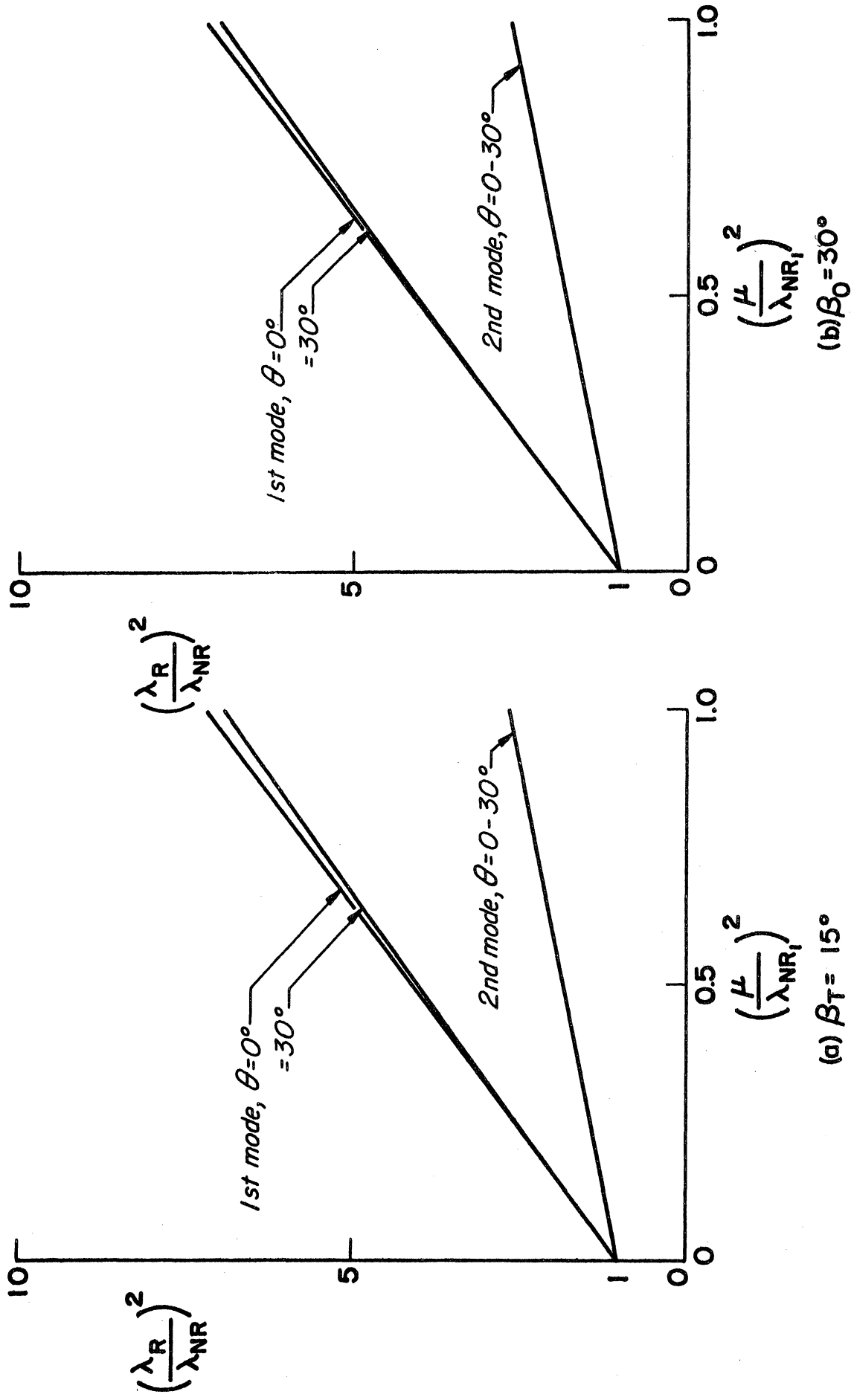


Fig. 17. Influence of twist on frequency ratios for rotating uniform articulated blade.  $\gamma^2 = 0$ ,  $\bar{e} = 0$ .



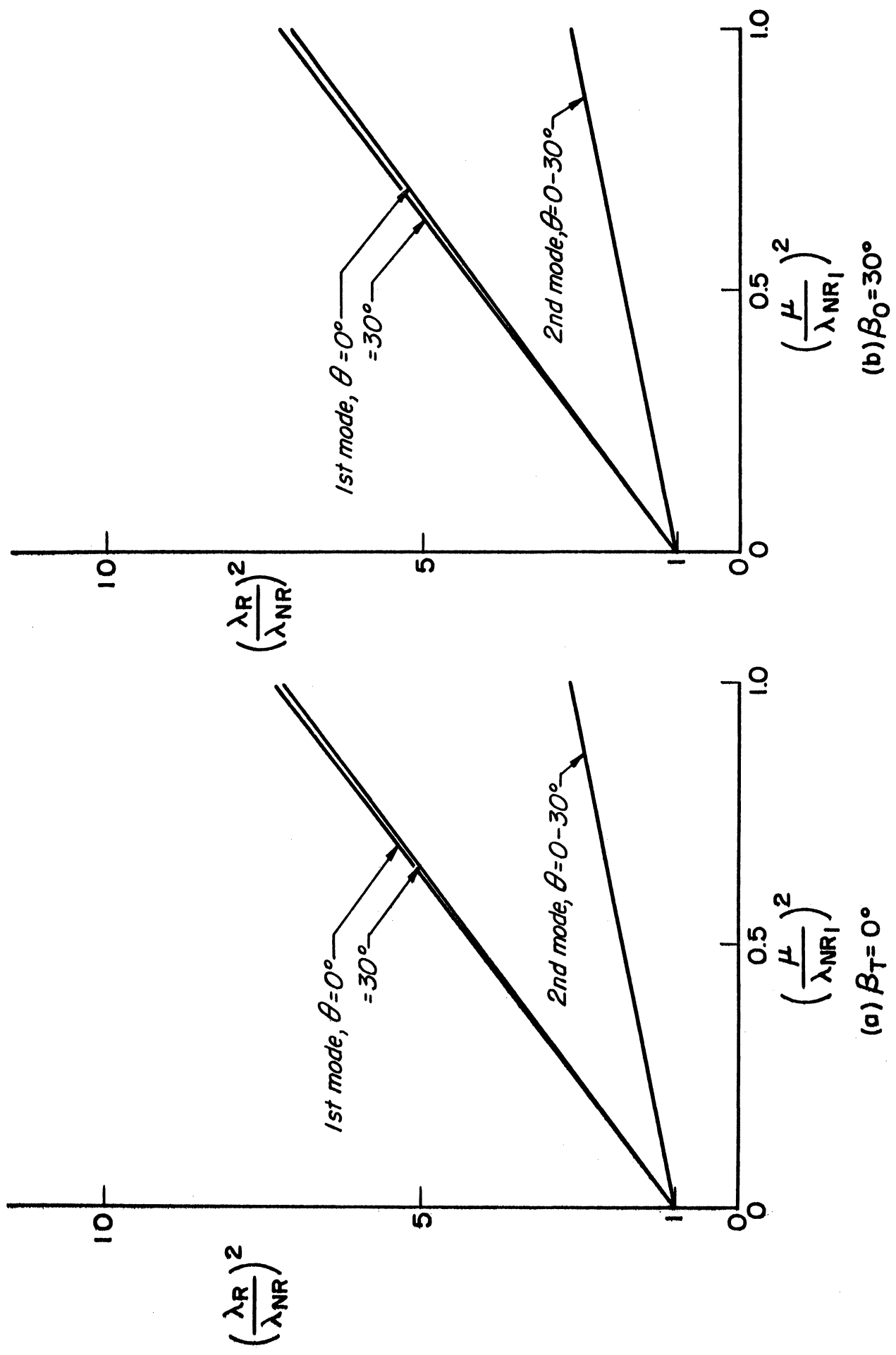


Fig. 18. Influence of twist on frequency ratios for rotating uniform articulated blade.  $\gamma^2 = 0.01$ ,  $\bar{e} = 0$ .

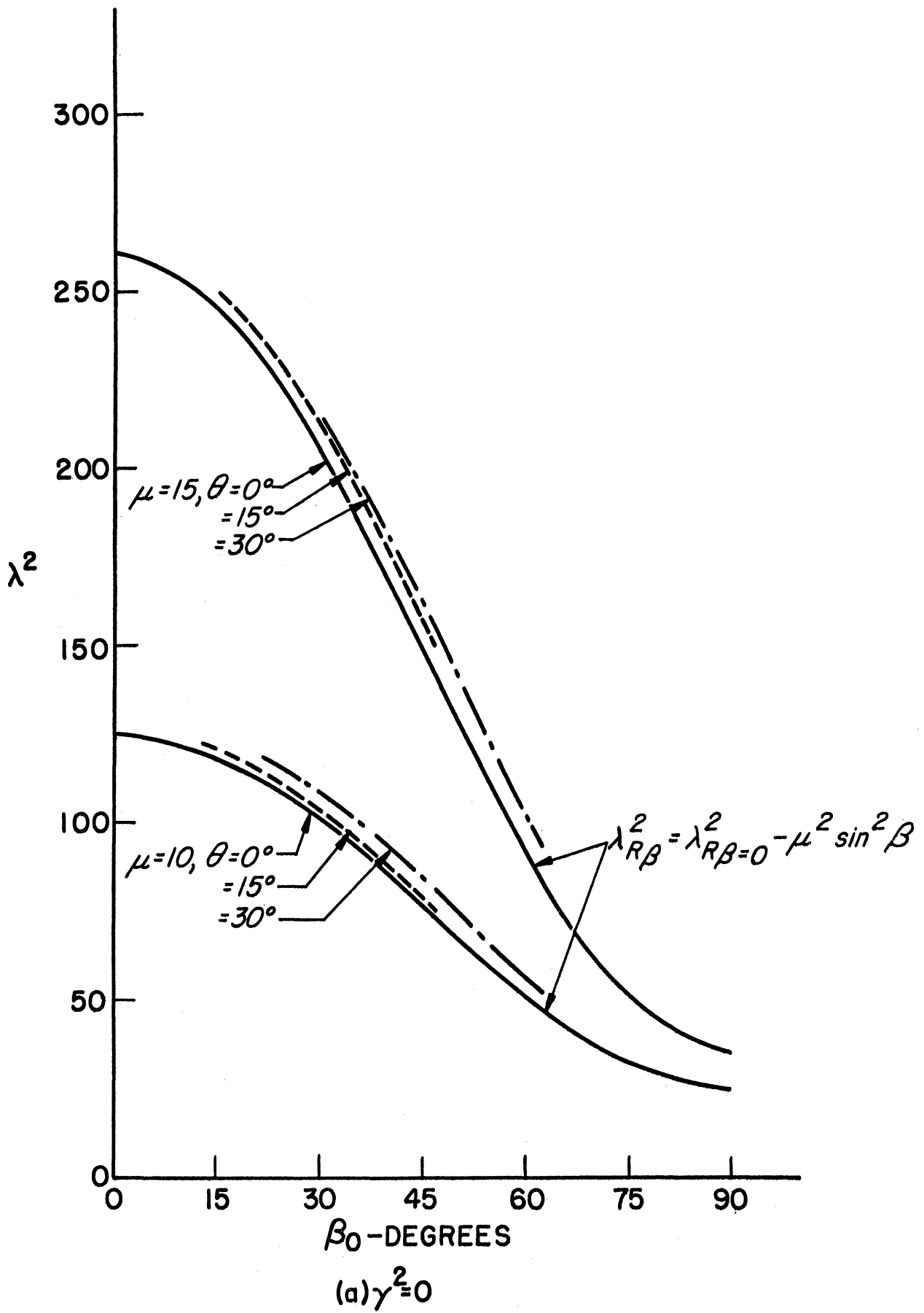
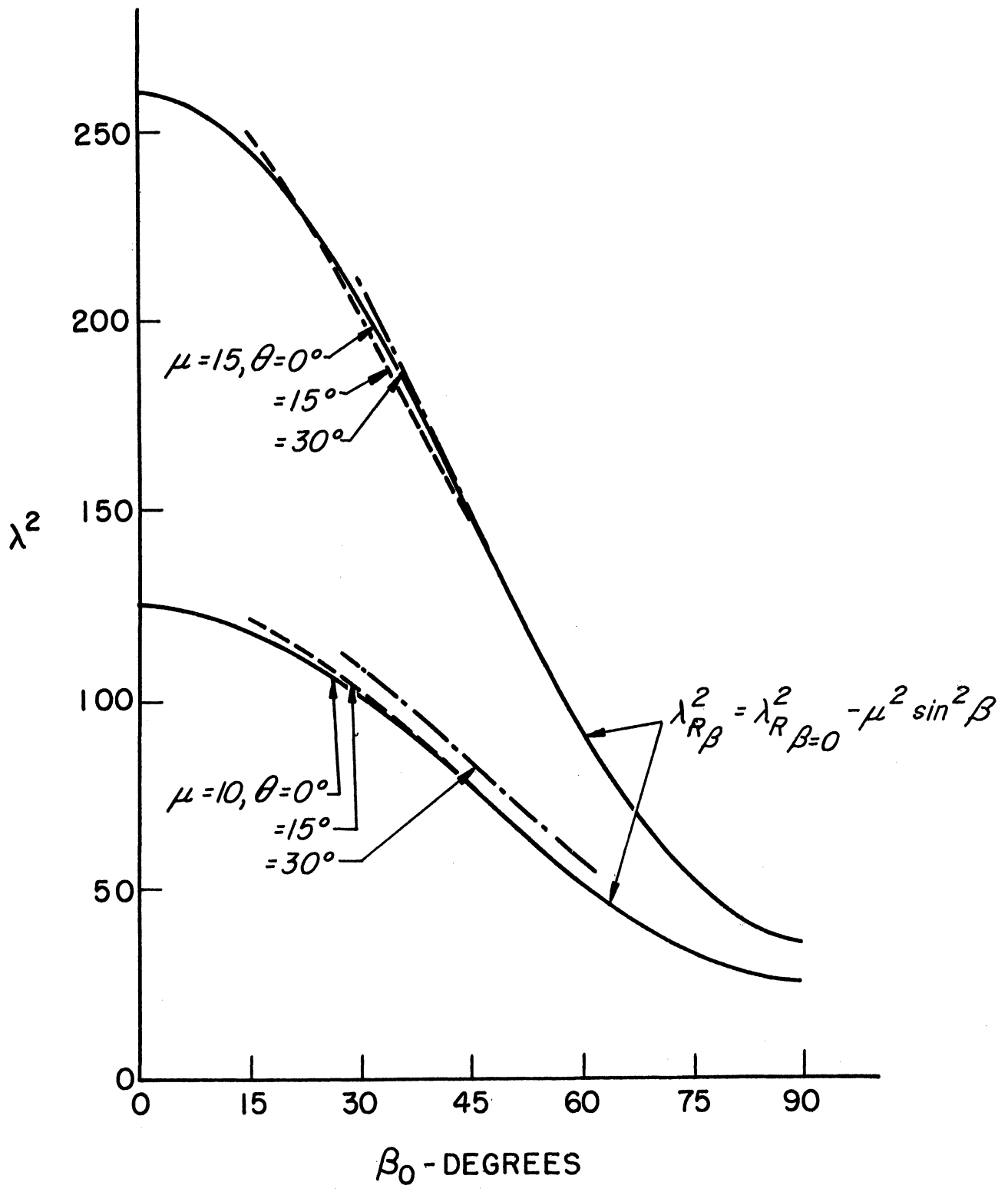


Fig. 19. Effect of root blade angle on fundamental frequency of uniform cantilever blade.



(b)  $\gamma^2 = 0.01$

Fig. 19. (Concluded)

